Mechanical Behavior of Layered Foam Composite Panels Subjected to Low Velocity Impact Events

by

Tianyi Luo

Presented to the Graduate and Research Committee

of Lehigh University

In Candidacy for the Degree of

Doctor of Philosophy

in

Mechanical Engineering

Lehigh University

January, 2016

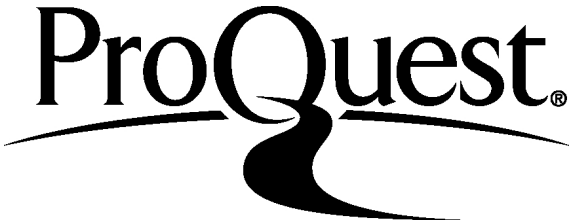

APPROVAL OF THE DOCTORAL COMMITTEE

"Mechanical Behavior of Layered Foam Composite Panels Subjected to Low Velocity Impact Events"

Approved and recommended for acceptance as a dissertation in partial fulfillment of the requirements for the degree of Doctor of Philosophy.

_____
Date

_____

Dr. Herman F. Nied
Committee Chairman and Dissertation Advisor
Department of Mechanical Engineering and Mechanics

_____

Dr. D. Gary Harlow
Department of Mechanical Engineering and Mechanics

_____

Dr. Edmund Webb III
Department of Mechanical Engineering and Mechanics

_____

Dr. Raymond A. Pearson
Department of Material science and Engineering

Acknowledgements

Looking back at journey in Lehigh Unversity, I feel I have been immensely fortunate to be able to work with a group of brilliant people. My deepest appreciation goes to Professor Herman F. Nied, my Ph.D. advisor, for introducing me to the field of my Ph.D. study and for his unwavering support and encouragement over the years. None of my accomplishments could ever be made without his inspiration and guidance.

I would like to thank all my Ph.D. committee members: Dr. D. Gary Harlow, Dr. Raymond Pearson, and Dr. Ed Webb III who gave me guidance and direction throughout my quest to obtain my Ph.D. degree.

To all the faculty and staff of Department of Mechanical Engineering and Mechanics: thank you. You have equipped me with the tools and information with which to pursue my career in Engineering. My special thanks go to Mr. William Maroun for always being helpful and insightful on my research. Many thanks to Dr. Xiao Liu for his kind help.

Most of all, I am extremely thankful to my beloved family, my parents and in laws. Specially, I feel deeply indebted to my wife Xi Chen. Without their unconditional love, inexhaustible support and encouragement throughout the past seven years, I could never go this far.

Contents

Contents iv

List of Figure vi

Abstract 1

Chapter 1. Introduction 3

1.1. Summary of the Dissertation 4

1.2. Background 5

1.3. Fiber Reinforcements with Polymeric Matrix 9

1.4. Low Modulus Closed-cell Foam 9

Chapter 2. Impact Performance Characterization 12

2.1. Evaluation Methods and Characterization 18

2.1.1 Characterization of Polymeric Matrix 19

2.1.2. Characterization of TPO/PVC Composite 23

2.1.3. Characterization of Polyisocyanurate Foam 25

2.2. Testing Methods to Layered Foam Composite Panels 27

Chapter 3. Low Velocity Impact Tests of Layered Foam Composites Panels 34

3.1. Strain-Rate Dependency Investigation 34

3.2. Effects of Composite Constituents 39

3.2.1. Effect of Fibers 39

3.2.2. Effect of Polymeric Matrix 42
3.2.3. Effect of Low Modulus Foam 45
3.2.4. Effect of Contact and Boundary Condition of the Layered Composites 51
3.3. Discussion and Conclusion 56
Chapter 4. Modeling and Simulations 57
4.1. Meso-Scale Model 57
4.1.1. Thermoplastic Polyolefin Properties/The Mooney-Rivlin Model 59
4.1.2. Numerical Model of Fabric Scrim 63
4.1.3. Crushable Foam Model 66
4.2. Finite Element Modeling 67
4.3. Roofing System Models 72
4.4. Boundary Condition Investigation 75
Chapter 5. Conclusions and Future Work 78
Bibliography 80
Appendices 83
Vita 84

List of Figure

Figure 1. The three axes of complexity [5] 8

Figure 2. Standard foaming process [11] 11

Figure 3. A) Polyurethane foam cell. B) Polypropylene foam cell [12] 11

Figure 4. Schematic of an impact event with a spherical projectile 12

Figure 5. Flowchart of the solution methodology 13

Figure 6. Schematic of a conventional split Hopkinson pressure bar with high-strength steel bars 15

Figure 7. Schematic of the modified split Hopkinson pressure bar with high-strength aluminum bars for testing low-impedance specimens [15] 15

Figure 8. Uniaxial tensile test to TPO membrane with fiber scrim reinforcement 16

Figure 9. Polyisocyanurate foam characterization – uniaxial tensile test 16

Figure 10. Polyisocyanurate foam specimen 17

Figure 11. Strip-biaxial tension experiment set up for PVC/TPO membrane 20

Figure 12. Uniaxial tensile tests to TPO/PVC membrane samples 20

Figure 13. strip-biaxial tension test 21

Figure 14. Stress vs. Strain Curves for Thermoplastic Polyolefin Samples 22

Figure 15. Force vs. extension Curves for PVC membrane samples 22

Figure 16. Thermoplastic polyolefin with fiber scrim reinforcement 23

Figure 17. Force vs. extension of PVC membrane with fabric scrim reinforcement ... 24

Figure 18. Uniaxial tension test to Polyisocyanurate foam dog-bone specimen 25

Figure 19. Experimental data of Polyisocyanurate foam non-linear stress-strain curve from uniaxial tensile/compressive tests 26
Figure 20. Spherical indenters used in lab measurement.....27
Figure 21. Load cell for quasi-static indentation tests 28
Figure 22. Instron Machine 8801 for dynamic indentation tests 28
Figure 23. Instron servohydraulic system 8801.....29
Figure 24. The testing rig, gas gun to launch the lab made ice-ball projectile 30
Figure 25. How the impact force measurement system works 31
Figure 26. Different configurations from single material structure to complex sandwich composites 32
Figure 27. Dynamic indentation test to Polyisocyanurate foam with 5/8" spherical indenter 37
Figure 28. Dynamic indentation test to Densdeck with ISO foam substrate (5/8" indenter).....38
Figure 29. Dynamic indentation test to TPO layered composite panel with 5/8" Indenter 38
Figure 30. Dynamic indentation test to TPO layered composite panel with 5/8" Indenter 39
Figure 31. Comparison of the size of indenter with the opening after perforation.....41
Figure 32. Indenter with flat head D = 9.5mm (left) with spherical head D = 15.9mm (right) 42
Figure 33. Stress vs. Strain curve of TPO membrane.....43

Figure 34. Transparent TPO membrane with fabric scrim reinforcement.....44

Figure 35. Fabric yarn slippage, red circle shows the tip of the pulled yarns 45

Figure 36. Typical foam stress-strain curve (quasi-static).....46

Figure 37. A schematic indicating the phenomena that occur during the three stages of plastic deformation in a cellular Al Alloy subject to compression [23] 48

Figure 38. Force vs. deflection curve of Polyisocyanurate foam board 50

Figure 39. Cross-section to the Polyisocyanurate foam in progressing stage of indentation tests. 50

Figure 40. Indentation test to layered foam composite panel with sliding & lifting behavior.....52

Figure 41. Experimental results: Adhered interface vs. Sliding & lifting interface 53

Figure 42. Free drop test of light spherical ball (24g) associated with 7.5 m/s impact velocity, arrows point at the maximum rebounce height of the spherical ball. 55

Figure 43. Free drop test of heavy spherical ball (560g) associated with 6 m/s impact velocity, arrows point at the maximum rebounce height of the spherical ball. 55

Figure 44. Experimental-FE correlation of PVC membrane with Mooney-Rivlin Model 62

Figure 45. Microscope Image of Fabric Scrim 63

Figure 46. Mooney Rivlin model with embedded shell elements (left), biaxial tension experimental test (right). 65

Figure 47. Experimental-FE correlation of PVC membrane with fabric scrim reinforcement biaxial tension result (in black) and numerical result (in red). 65

Figure 48. Experimental data of foam stress-strain curve for crushable foam model ..66

Figure 49. Typical foam model results vs. experimental test data with controlled indentation.....67

Figure 50. Partial View of 3-D Finite Element Model 69

Figure 51. Experimental indentation test to the layered structure with sliding & lifting contact 71

Figure 52. Simulation results in ANSYS Explicit Dynamics 71

Figure 53. Rigid board: densdeck (left), HDboard (right) 73

Figure 54. Layered composites panels structures from complex to simple 74

Figure 55. Indentation failure mode of ¼ symmetry model, TPO membrane layer top view (left) and TPO membrane layer side view (right) 74

Figure 56. Boundary condition setup in FE modelling.....76

Figure 57. numerical modeling results of light weight ball (24g & 0.66J Impact Energy) free drop impact to layered TPO/foam panel.....77

Figure 58. numerical modeling results of heavy weight ball (240g & 4.2J Impact Energy) free drop impact to layered TPO/foam panel.....77

Abstract

A layered foam composite panel system has higher moment of inertia, therefore increasing its bending stiffness. A low modulus backing material in the layered composite panel could provide energy absorption capability when an impact event occurs. These feature make the structure system very promising in many engineering field such as energy absorption, aerospace and automotive. Polymeric and textile reinforcements can be used to form a large deformable structure with closed-cell foam substrate together. The mechanical behaviors of such materials, including the thermoplastic polyolefin membrane, reinforcement scrim, low modulus closed-cell foam and fiber-glass stiffened facer sheets, were characterized and exanimated at controlled velocity indention and impact conditions.

A finite element model is developed to simulate dynamic stress distributions in layered foam composite panels subjected to severe impact events, e.g., hail and hard object strikes. In order to build an integrated layered foam composite panel model, separate sub-models are developed that include: the polymeric matrix membrane, reinforcement scrim, low modulus closed-cell foam and fiber-glass stiffened facer sheets. A Mooney-Rivlin model of the polymeric matrix membrane is utilized to simulate the membrane's large-deformation mechanical response during simple impact tests. The failure mode and criterion of each individual component in this layered foam composite system had been evaluated and quantified. Straightforward force-contact measurements on the reinforced polymer membrane composite material and low

modulus foam backing, using spherical indenters, are shown to provide sufficient material properties for the impact model of interest. It is demonstrated that the local failure modes for the layered foam composite system can be characterized by using relatively simple failure criterion for each of the individual component layers in this type of system. Excellent correlation is obtained between model predictions and experimental dynamic impact/indentation tests.

Chapter 1. Introduction

In many advanced engineering applications, layered composites have been used due to their high strength, high energy absorption capability, and light weight. The dynamic behavior of such laminated "crushable" polymeric composites are of considerable practical interest. The structure's integrity can be can drastically altered by foreign object impacts, The structure's integrity can be can drastically altered by foreign object impacts, e.g., hail stones, or dropped tools. The integrity of a layered structure under impact events is critical for many applications, from the manufacturing of space shuttle, airplane, automotive, to the design of personal protection gear. The integrity of the structures under impact events brought the attention of researchers. NASA Glenn Research Center studied and evaluated the damage when a foam material as a projectile striking to the carbon-reinforced composites. The energy absorption capability of the layered structure could benefit the design of personal protection vests or helmets, and many other applications. Another example is highway or high speed race-track barriers could be improved by utilizing such layer composite structure with high energy absorption capability. A thorough, quantitative understanding of all the mechanisms during the ballistic impact into fabrics and composites is still learned through experimental tests, observations, and discussion from modeling efforts. Since there are a number of complex interactions effecting the layered composites performance during the impact event occurs, the quantitative understanding of all the dominant mechanisms during the dynamic event is best understood through a combination of experimental

tests and finite element simulations. A general description of the impact deformation phenomena will be introduced next.

1.1. Summary of the Dissertation

In general, the introductory chapter includes a literature survey overviewing layered foam composite materials with an in-depth examination and characteristics of reinforced polymeric hyperelastic materials and polyisocyanurate foam. **Chapter Two** introduces the mechanical testing methods and the explanations of the setup of the impact testing rig including indentation test with variety indentation velocity, and dynamic impact test. **The Third Chapter** will examine impact performance characterization information regarding techniques available, evaluation techniques and how the components of the layered foam composite panel affect the performance of the material. The post-impact results can be found in this chapter. **The Forth Chapter** details the materials model and finite element definitions for the formation of the low velocity impact event to layered composite panels. The simulations of dynamic indentation and impact were analyzed and discussed. Finally, the work included in this dissertation is summarized and the contributions of the dissertation are concluded. Future work of this research is also expected in the final chapter.

1.2. Background

Due to the excellent mechanical properties like high strength, stiffness, lightweight, energy absorption capability, and increased fatigue life among others, the layered composites subject to the impact event have been investigated by many researchers. In general terms, a composite is a multiphase material comprised of two or more distinct materials that combined result in possession of a better combination of the physical properties of each of its constituents [1]. The layered foam composites may consist of hard layer(s) backed by ductile, energy absorbing layer(s). Typically, the hard layer(s) consists of ceramics, steel, aluminum, or polymer matrix. In the case of polymer matrix composites, the matrix is a polymer of some variety and the interface layer is often a fiber or particle reinforcement.

As a starting point to describe the impact event into layered foam composite panels. The impact into a single fiber will be described first. The high-strength, high-modulus fibers, bundled into yarns, has been able to develop the impact resistant fabrics and compliant laminates. When impacted, the stress on the yarns has a sharp increase, and the value of the stress depends on the impact velocity. When the impact velocity is sufficiently low, the stress increase is not high enough to rupture the fibers, therefore allows the transverse deflection and yarn extension propagate, resulting in the absorption of energy by the fibers [2]. Fibers possessing high-tensile strength and large failure strains can absorb a big amount of energy. Lee, *et al*. [2] correlated the number of yarns broken to the levels of impact energy absorbed and stated that the fiber straining

is the primary mechanism of the energy absorption in the penetration failure of ballistic textiles.

Many researchers have conducted modeling to study the influence of material tensile properties on the high-speed impact performance. However due to the lack of high strain-rate properties, most of the studies are using the static properties of the material. Lim, *et al*. [3] have developed a three-element viscoelastic representation for the rate dependent modulus of the aramid fabric Twaron. They modeled the fabric as a strain rate dependent isotropic elastic-plastic material with dynamic finite element software LS-DYNA.

Although tensile strength, modulus and strain-to-failure of a yarn play an important role in impact performance, each property itself does not play a dominant role. Cunniff [4] has derived a dimensionless fiber property defined as the product of the specific fiber toughness multiplied by its strain wave velocity.

$$U^* = \frac{\sigma\varepsilon}{2\rho}\sqrt{\frac{E}{\rho}} \qquad (1\text{-}1)$$

where σ is the fiber ultimate tensile strength, ε is the fiber ultimate tensile strain. The relationship between the mechanical properties of individual property and the impact resistance of a layered composite panels is very complicated and there are many factors that influence the impact performance of the overall system.

A global optimization technique with finite element (FE) based impact simulations has been produced by many researchers. By presenting experimental characterization of

individual materials, experimental-FE comparisons and validations. In general, three factors, in the modelling and optimization work, have been described as the three axes of complexity. They are analysis complexity, model complexity, and optimization complexity [5].

The simulation of the impact events is a non-linear response due to the complex interaction of material damage and system response. For Lagrangian simulation techniques, the non-linear deformation process requires short time steps when explicit algorithms are used. It may be necessary to use a fine mesh to capture the rapidly varying stress distributions and strain gradients. While dealing with non-linear strain-rate sensitivity material models, thickness variations, number of layers, simple 2-D geometries to complex 3-D structures, it's at the peak of the axes of complexity. [5].

To validate the simulation for reality representation, it's necessary to check qualitative and quantitative measurements, such as residual kinetic energies, deformation sizes, and damage modes. Numerical instabilities can appear due to the contact logic and highly distorted elements in the simulations. The modelling process typically requires user-intensive interaction to comparing experimental results with model predictions. During the simulation, it's significant important to apply engineering experience to assess the physicality of the observed phenomena.

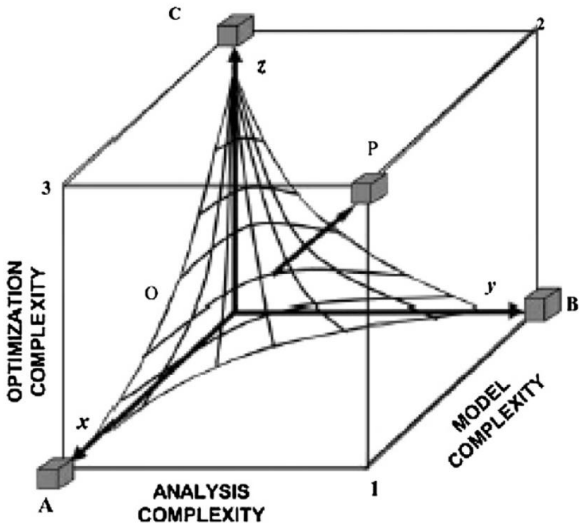

Figure 1. The three axes of complexity [5]

One of the most important testing procedures is about recreating the impact events, which can be divided into low-velocity, high-velocity and ballistic impact conditions. In this dissertation, low velocity impact tests were produced and simulated by finite element model. Since the velocity is not constant during the impacting process, the quasi-static and dynamic results may not be compared directly. However, the speed reduction is important in the densification phase where the force and deceleration are continuously growing. When the impact event occurs, the substrate material was deformed at the local spot contacted with the spherical indenter. Multiple dis-similar materials could be combined together to sustain the impact load, which makes the system very unique but can be varied at different applications.

Due to the highly dissimilar material properties of the layered composites structure, some interesting comparisons can be done among the tests of thickness variation,

interface bonding variation, deformation at differed strain rate, and composite material selections. The variation of boundary conditions could impact the simulation results and failure modes significantly. All these challenges are investigated and discussed in the following chapters.

1.3. Fiber Reinforcements with Polymeric Matrix

The layered foam composites may consist of hard layer(s) backed by ductile, energy absorbing layer(s). Typically, the hard layer(s) consists of ceramics, steel, aluminum, or polymeric matrix. In the case of polymeric matrix composites, the matrix is a polymer of some variety and the interface layer is often a fiber or particle reinforcement.

Polymeric composite materials are being explored in the medical field. Ramakrishna, *et al*. [6] explore the development of a thin and flexible composite material for biomedical applications using polyester fiber interlock fabric as reinforcement and polyurethane elastomer as the matrix. The effect of pre-stretching of the fabric has been identified on the composite tensile properties. Ramakrishna, *et, al* state that both the stiffness and strength of composite improved in the direction of fabric pre-stretch and deteriorated in the direction normal to pre-stretch.

1.4. Low Modulus Closed-cell Foam

Synthetic cellular materials play an important role in many passive safety applications, for packaging, cushions, automotive, aerospace and so on. These materials have low cost, light weight, and high workability. Metallic foam, though less common,

is also synthetic cellular material with discrete gas cells separated by thin metal membranes [7,8].

The mechanical performance of closed-cell foams is important for the applications, such as cores for sandwich composites, crash/blast energy absorbing systems [9,10]. One of the most important properties is the energy absorption capability governed by elastic stiffness, the yield strength and the plateau stress. Energy is dissipated through the cell wall buckling or fracture, but the plateau of the stress strain curve usually limits the stress. The shape of the protective structure also influence load transfer during impact, and the capacity to absorb elastic energy, which in turn controls rebound.

The mechanical performance of closed-cell foams is important for applications, such as cores for sandwich composites, crash/blast energy absorption and so on [11]. These enhanced energy absorption capabilities and lightweight make these cellular foam materials highly desirable compared with traditional materials such as metals. The Polyisocyanurate foam has closed-cell structure, which could be highly distorted under deformation. The study on this kind of material shows us how the energy is absorbed and then transferred to its structure. Energy is dissipated through the cell wall buckling or fracture, but the plateau of the stress strain curve usually limits the stress [12]. Therefore, with the high specific stiffness and impact energy absorption, the foam structure can be utilized to prevent a projectile all the way through itself, which is one of its great potential to improve safety.

The study on this kind of material shows us how the energy is absorbed and then transferred to its supporting structures. Energy is dissipated through the cell wall

buckling or fracture, but the plateau of the stress strain curve usually limits the stress. The shape of the protective structure also influences load transfer during impact, and the capacity to absorb elastic energy, which in turn controls rebound. Therefore, with the high specific stiffness and impact energy absorption, this foam structure can be utilized to prevent a projectile all the way through itself, with demonstrates its great potential to improve safety.

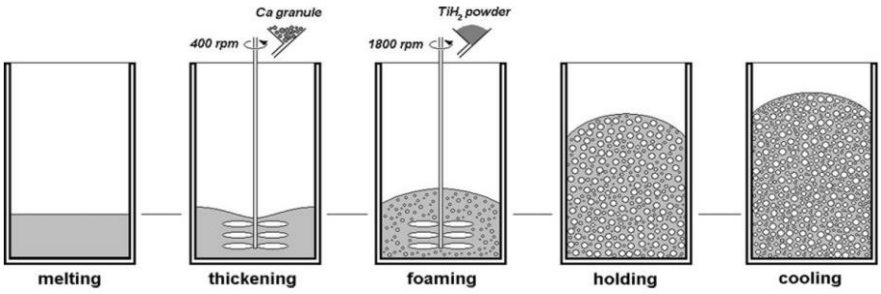

Figure 2. Standard foaming process [11]

In addition, the characterization of polymeric foam for roofing construction, will be significantly promising, because of its features of thermal insulation, energy absorption and light weight. For example, the thermal insulation feature can save the energy loss of household, which provides a more efficient method to use energy.

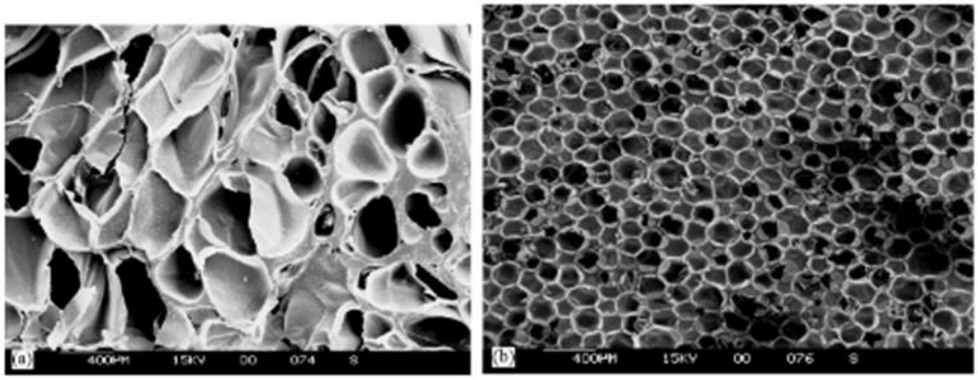

Figure 3. A) Polyurethane foam cell. B) Polypropylene foam cell [12]

Chapter 2. Impact Performance Characterization

The objective of this research is to characterize the impact behavior of the layered foam composite material, to examine the feasibility of applying such materials for impact events to enhance the integrity of the structure. The proposed layered foam composite panel includes soft polymeric matrix covering layer and high-energy absorption capability foam backings.

In the present work, experimental measurement of impact deformation will be compared against the numerical values from the impact model using the finite element analysis package ANSYS. One challenge for the numerical simulation is the characterization and measurement of material properties. During the impact events the strain rates can be the order of $10^2\ s^{-1}$ which is significantly higher than the loading rates when material properties are measured. Some effort will be applied to validate the properties measurements and then provide the confidence in using them in modeling the impact events.

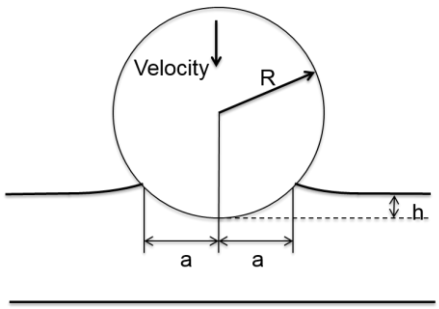

Figure 4. Schematic of an impact event with a spherical projectile

Figure 5 shows the geometry of spherical indentation. The sphere of radius *R*, has a normal velocity *u*, producing a contact radius *a* and indent depth *h*. if the material piles up above the initial surface of the half-space, the pile-up is positive [13].

A flowchart of the model and experiments can be drawn and summarized as follows:

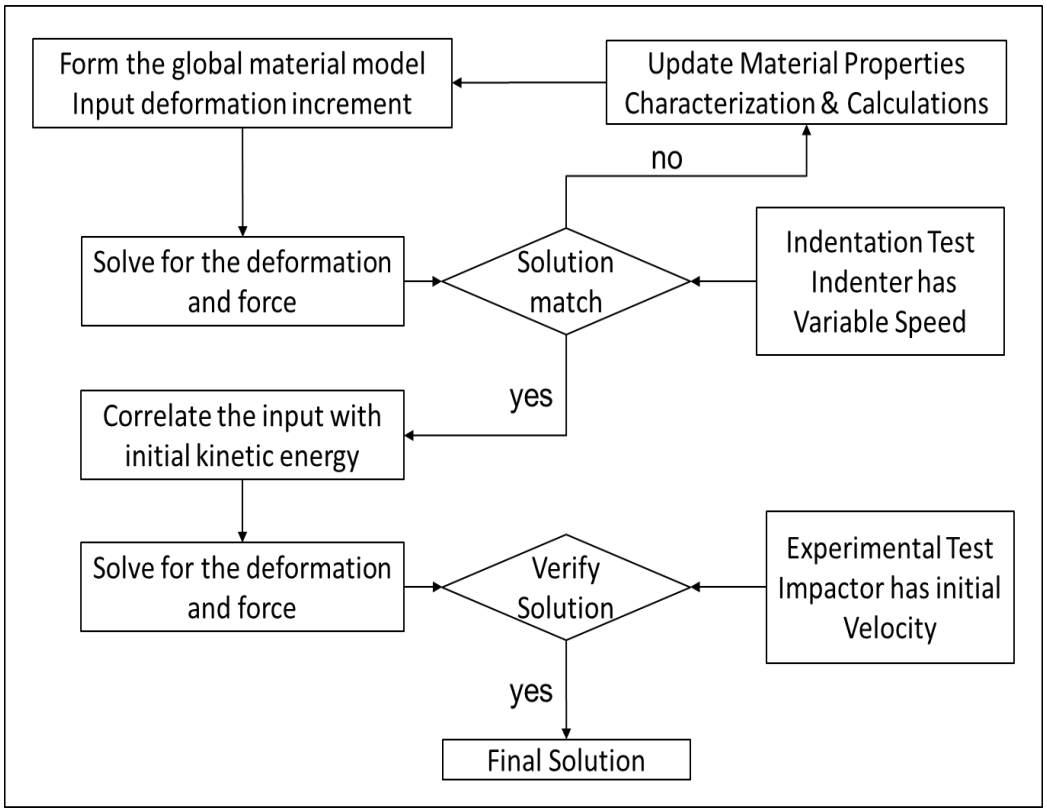

Figure 5. Flowchart of the solution methodology

The technical approach for this problem is as follows:

- Test a variety of materials and configurations in order to characterize their mechanical behavior during the impact event.

- Characterize the materials constituent properties and calibrate the parameters in low velocity dynamic indentation tests.
- Carry out impact tests using a gas gun from GAF, which can accelerate the impactor to different velocities, up to 40m/s.
- Employ a high-speed camera in order to capture the deflection and rebound that occurs to the layered composites and impactor. A dynamic load cell can be used to get the reaction force data.
- Create a finite element model to depict the impact and deformation interactions.
- Compare predictive and experimental solutions.

In order to measure the high strain rate materials parameters, the conventional split Hopkinson pressure bar, shown in Figure 6, is commonly used for metal materials. However it has serious limitations to measure the materials with low strength and low impedance. Zhao, *et al*. [15] developed an experimental technique that modified the conventional split Hopkinson-bar for reliably and accurately measuring the compressive stress-strain responses of materials at high strain rates. The test specimen, which has low mechanical impedance and low compressive strength, was bonded between an incident bar and transmission bar. Avalle *et,al.* utilized a drop dart machine to accomplish the test [14]. The machine has a mass of 20kg and a maximum drop height of 2m.

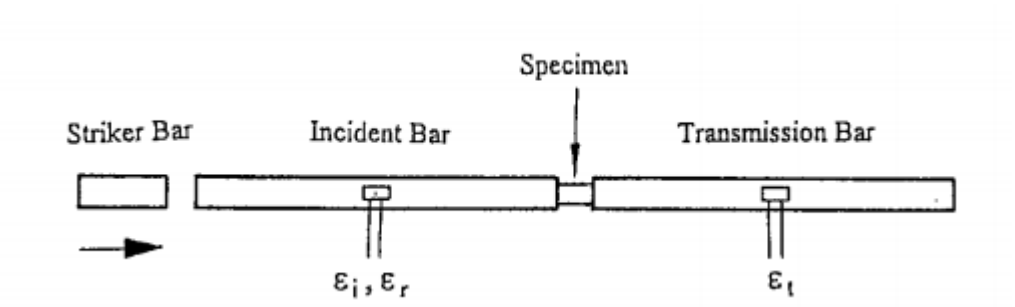

Figure 6. Schematic of a conventional split Hopkinson pressure bar with high-strength steel bars

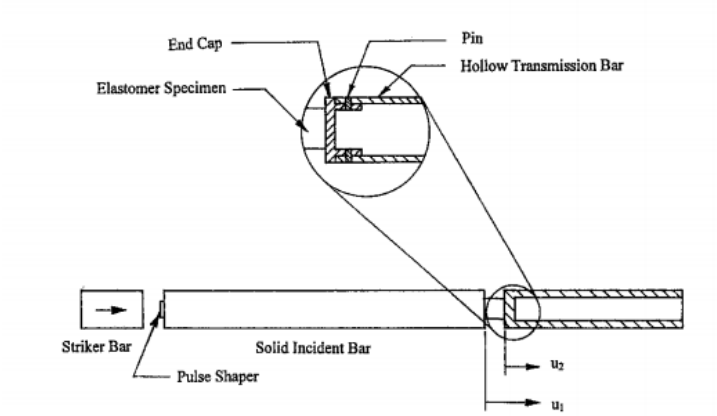

Figure 7. Schematic of the modified split Hopkinson pressure bar with high-strength aluminum bars for testing low-impedance specimens [15]

An important part of the tests is to determine which composite constituents have the greatest effect on the impact performance of the layered structure. A detailed look and examinations are necessary by break each constituent down for the effect and failure mechanisms. For instance, a TPO composite with fiber scrim reinforcement can be considered as three main constituents: the matrix, the fiber scrim, and the bonding interface. The examination can provide important references during the modeling work.

In order to measure the material parameters of polymeric matrix materials, such as thermoplastic polyolefin membrane, or PVC membrane, a structure shown in Figure 8

Can be used as the fixture implementation to the Instron machine. The pre-cut membranes are weaved through the slots and provide the lock feature. This lock feature coming with a high friction force holds the samples during the process of axial tensile tests. A 10kip load cell is utilized in this soft membrane characterization. Due to the design of the fixtures with weaving slots, the maximum tension load is 4,400 N (approximately 1000 lbf). Although the material at the lateral edge will deform due to the lateral loading, the material doesn't deform in the center. Therefore, the so called strip-biaxial tension stress vs. strain curve can be captured by this testing manner.

Figure 8. Uniaxial tensile test to TPO membrane with fiber scrim reinforcement

Figure 9. Polyisocyanurate foam characterization – uniaxial tensile test

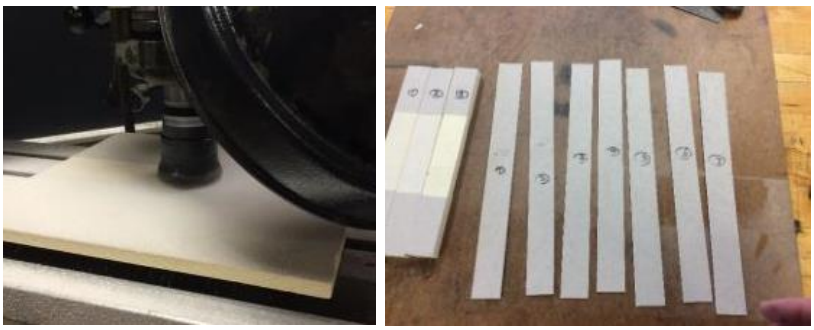

Figure 10. Polyisocyanurate foam specimen

The procedure to characterize the materials parameters at lower strain rate is well established. Hence, it's important to explore and research that whether or not the material parameters measured in quasi-static condition can adequately represent the actual structural behavior at higher strain rate. Thus, one measurement method in this work is performing and correlating the materials parameters in both quasi-static and dynamic loading conditions. A 10Kip screw-driven Instron machine can perform the indentation test up to 500 mm/min. The uniaxial tensile/compressive tests are produced by the 10Kip screw-driven Instron machine to provide the quasi-static material properties of each constituent of the layered composite samples. Figure 8-10 show the uniaxial tensile experiments to characterize the materials parameters.

Although the actual testing of layered foam composite panels under impact events will be carried as part of this study, the amount of testing to improve the modeling accuracy can be very high. Therefore, the material characterizations are necessary to obtain the physical material parameters. Then the impact tests will be used to provide the fundamental knowledge of the energy absorption, deflection and verify the

numerical modeling results. The results from the models will be used to compare with the experimental results. The permanent damage spot, deformation and/or delamination in the test panels will be selected as the damage criterions. The first is to measure and characterize the permanent deformation and the depth of the indentation. This will allow for further verification of the finite element models. The second method that can be applied is using Optical Microscope that is available at Whitaker in order to characterize the failure modes in the test specimens if needed.

2.1. Evaluation Methods and Characterization

In this study, there are three basic material constituents: PVC/TPO polymer, fabric yarn scrim, Polyisocyanurate foam. Each of them are measured for their physical parameters. The simple tension/compression tests, including uniaxial compression, strip-uniaxial tension, strip-biaxial tension test, are carried in the lab for the fundamental physical parameters measurements.

Table 1. Test methods applied for material component

	uniaxial compression	strip-uniaxial tension	strip-biaxial tension
PVC membrane		✓	✓
PVC composite			✓
TPO membrane		✓	✓
TPO composite			✓
Polyisocyanurate foam	✓	✓	

high density Polyiso foam	✓	✓	

2.1.1 Characterization of Polymeric Matrix

Polymeric matrix, which are ductile, energy absorbing layer(s), are characterized with strip-uniaxial and strip-biaxial tension tests to obtain its mechanical behavior during the large scale deformation. For simulation purpose, the data will be transferred to hyperelastic Mooney-Rivlin model in the finite element code to capture the mechanical behavior of the Thermoplastic Polyolefin layers.

Because of these material has a tendency to elongate to a large value in loading direction and a corresponding reduction in the transverse modulus, a strip-biaxial tension test should be introduced as shown in Figure 11. Obviously, the material components along the edge are pulled toward the center and suffered with the non-zero loading in the transverse of loading direction, however the inner material components could be assumed to have zero loading in the transverse direction. Two geometry size of specimens are prepared which are 2.5" (length) × 0.75"(width) and 3" (length) × 6" (width) for strip-uniaxial tension, and strip-biaxial tension, respectively. The measured stress vs. strain from the TPO membrane tension test is shown as Figure 14. The stress of strip-biaxial tension test will increase slightly as the specimen width-length ratio increases. This biaxial tension test leads to an improved tensile modulus and strength of a TPO composite laminate. In general, the tensile responses of TPO membrane have the same trend between the strip-biaxial tension test and strip uniaxial tension test, given with the specimen width-length ratio of strip-biaxial tension test is 3:1.

Figure 11. Strip-biaxial tension experiment set up for PVC/TPO membrane

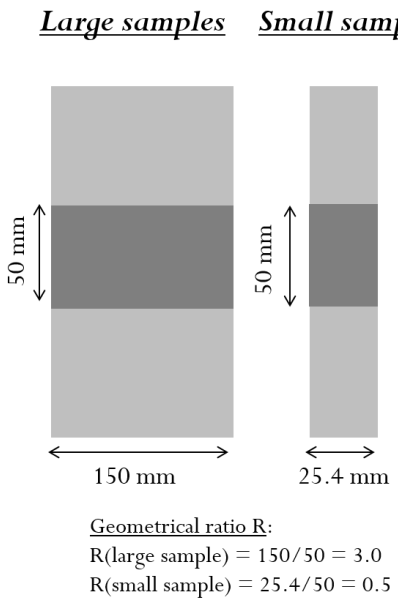

Figure 12. Uniaxial tensile tests to TPO/PVC membrane samples

Figure 14 shows the testing results to Thermoplastic Polyolefin (TPO) membrane under uniaxial tensile test. At the early stage of the tension test, the TPO specimen has a linear elastic response which is shown in the stress strain curve until the strain reach up to 50%. For both large width-over-length test and small width-over-length test, while

the specimens sustain with a transverse load and deformation, the slope of the stress vs. strain curve slowly decreases. However, in the large width-over-length test, the tensile stress of the specimen is higher than the stress small width-over-length test.

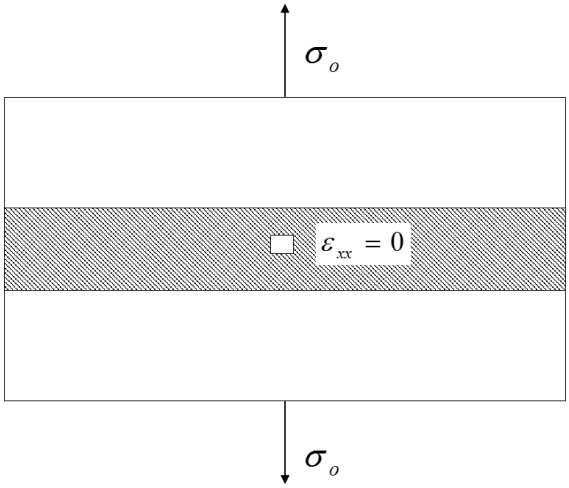

Figure 13. strip-biaxial tension test

$$\varepsilon_{xx} = \frac{1}{E}(\sigma_{xx} - \upsilon(\sigma_{yy} + \sigma_{zz})) \tag{2-1}$$

$$\sigma_{xx} = \upsilon\sigma_{yy} \tag{2-2}$$

$$\varepsilon_{yy} = \frac{1}{E}(\sigma_{yy} - \upsilon\sigma_{xx}) \tag{2-3}$$

$$\varepsilon_{yy} = \frac{1-\upsilon^2}{E}\sigma_{yy} \tag{2-4}$$

$$\sigma_{yy} = \frac{E}{1-\upsilon^2}\varepsilon_{yy} \tag{2-5}$$

where σ_{yy} is the stress component in loading direction and σ_{xx} is in transverse loading direction. At the center region $\varepsilon_{xx} = 0$, therefore the stress component σ_{xx} in the high width-length ratio tension test is a fraction of σ_{yy}, which makes it a biaxial

tension testing condition. For the specimen with small width-length ratio, the stress component σ_{xx} is zero, and $\sigma_{yy} = \sigma_o$, which makes it a strip-uniaxial tension testing condition in the center region.

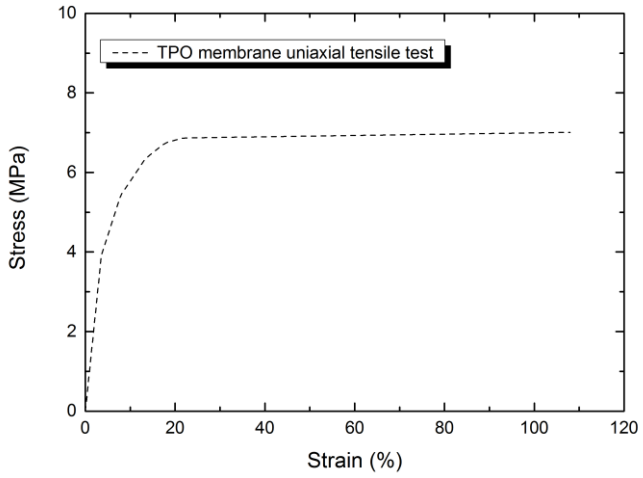

Figure 14. Stress vs. Strain Curves for Thermoplastic Polyolefin Samples

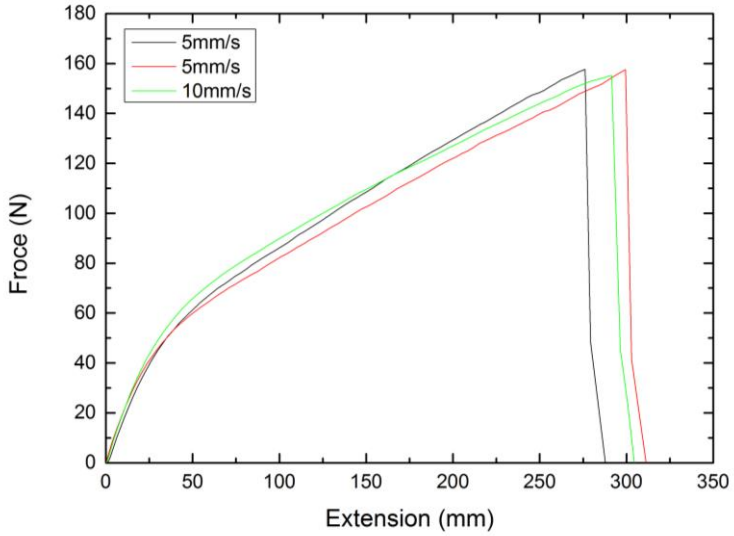

Figure 15. Force vs. extension Curves for PVC membrane samples

2.1.2. Characterization of TPO/PVC Composite

The TPO/PVC composites are provided by the roofing company GAF Materials Corporation for the commercial roofing system applications. The production method for the roofing composite employs a co-extrusion technique in order to adhere two different layers but the same kind of TPO or PVC together with a fabric reinforcement scrim between them. An example of half of this configuration, TPO layer, can be seen in Figure 16. Some sample sheets of TPO and PVC cap without fiber scrim reinforcement are also provided for material parameters measurements.

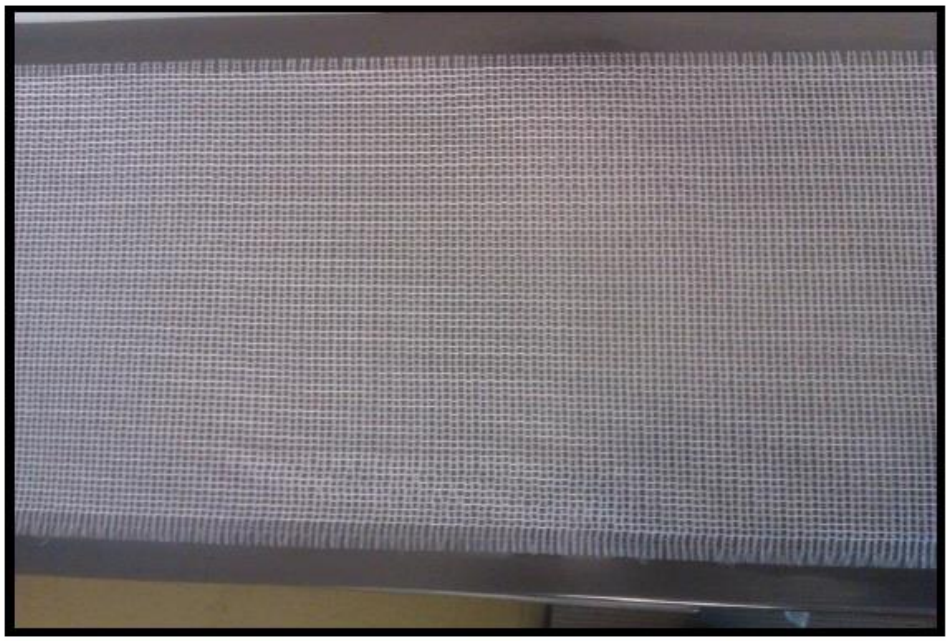

Figure 16. Thermoplastic polyolefin with fiber scrim reinforcement

Since it's not quite applicable to measure the mechanical behavior of fiber reinforcement scrim separately due to the complexity of the contact behavior and the lack of the scrim structural stability, the overall TPO composite biaxial stress-strain

curve are measured and used for the finite element model. Considering the contact behavior between the polymer matrix and the fiber reinforcement scrim, it might behave quite different between the low strain rate deformation event and impact events. Therefore, it's necessary to capture the differences at differed strain rates for material characterization.

The PVC composites with fiber scrim reinforcement are tested with the same width-over-length ratio as discussed in last section as strip-biaxial tension test. The stress vs. strain curve is shown in the Figure 17. The stress has a sharp increase when the value of strain goes over 75%.

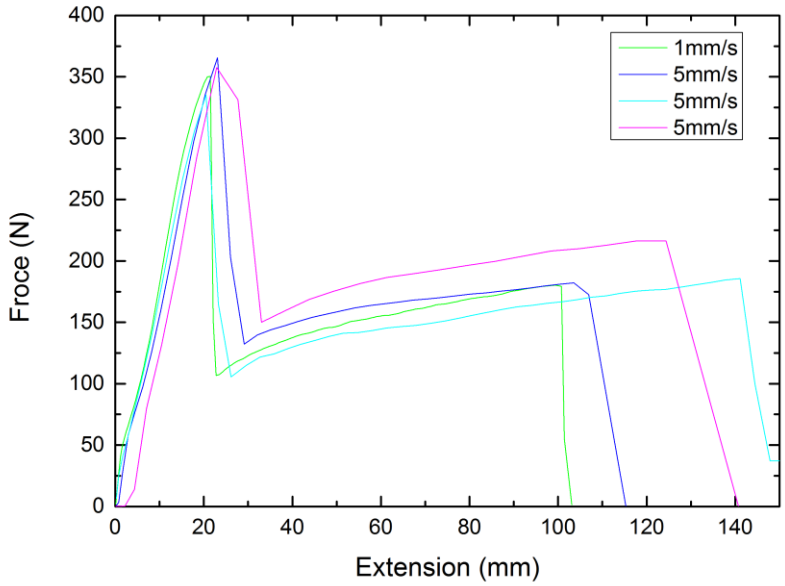

Figure 17. Force vs. extension of PVC membrane with fabric scrim reinforcement

2.1.3. Characterization of Polyisocyanurate Foam

The closed-cell foam material contributes to the impact absorption capability with its unique cell structure. The straightforward uniaxial tension and compression tests were performed to obtain the material parameters. Although the recommended sample geometry is dog-bone cylinder as the ASTM rigid foam tensile test standard, it's extremely difficult to cut the sample into cylinder manner due to the foam cell structure and its low strength. The tested dog-bone samples are cut by CNC waterjet in order to minimize the major defects on the surface. Since the test sample has low density and strength, wood blocks, which glued to the end of the foam samples, are applied as the gripers for the uniaxial tensile tests. The same testing manner with different sample geometry is applied to the uniaxial compressive test. Figure 18 shows the experiment set up and the shape of the specimen.

Figure 18. Uniaxial tension test to Polyisocyanurate foam dog-bone specimen

A typical compression/tension stress vs. strain curve for the Polyisocyanruate closed-cell foam is shown as Figure. The measured stress vs. strain in compression initially

exhibits a linear elasticity behavior due to the cellular wall elastic bending. It has a significant similarity with the behavior in tension when the strain is less than 5%. After this point, the tangent modulus decreases rapidly with strain increasing and followed by a plateau region of strain softening corresponding to cell wall bucking or plastic yielding. This force vs. displacement behavior can be verified by quasi-static indentation test and finite element model in chapter 4. The uniaxial compressive test didn't approach to the densification stage and the semi-empirical estimation would be produced to the finite element model.

In the tension side, a linear elasticity behavior can be seen until the foam specimen fails abruptly at the start location of the necking area. Thus, it provides the tensile ultimate strength of the specific macro-scale foam material and will be used as the cutoff value of the foam model in FEM. A similar stress-strain behavior also has been found when testing the high density closed-cell foam sample.

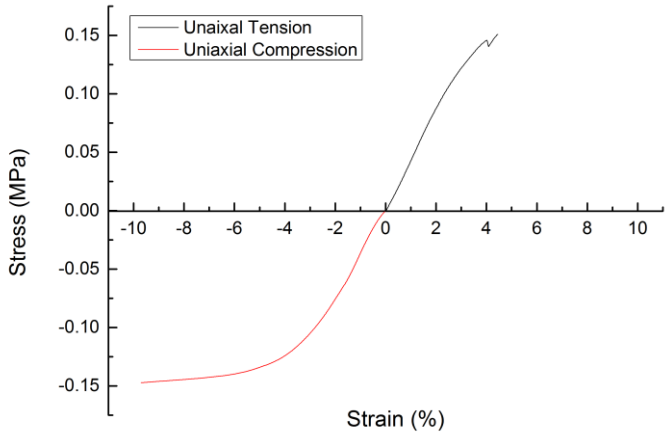

Figure 19. Experimental data of Polyisocyanurate foam non-linear stress-strain curve from uniaxial tensile/compressive tests

2.2. Testing Methods to Layered Foam Composite Panels

In order to characterize the performance of a composite, a variety of tests need to be performed. In this work, the experiments are running at different indentation velocity from 0.25 mm/s to 70 mm/s in order to compare the data at a variety of strain rate and estimate the strain rate effect to the system. A 25.4 mm × 25.4 mm test specimen with 50 mm thickness is placed on the test area. The indenters with a variety of diameter are manufactured by welding spherical a steel ball to the rod with thread. The welded indenter is utilized to mimic the rigid spherical projectile.

Figure 20. Spherical indenters used in lab measurement

Figure 21. Load cell for quasi-static indentation tests

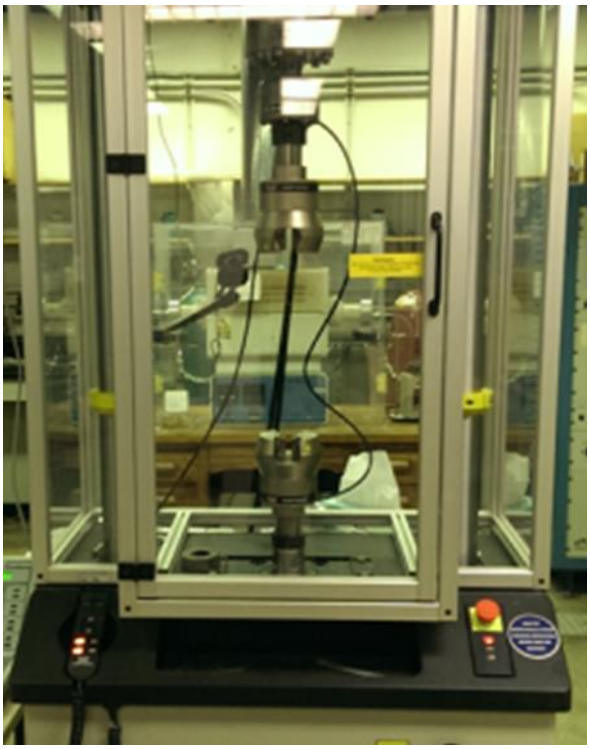

Figure 22. Instron Machine 8801 for dynamic indentation tests

The Instron 8801 is a compact servo hydraulic fatigue testing system that meets the demands of various static and dynamic testing requirements. It has double-acting servohydraulic actuator with force capacity up to 22Kip. The Instron system 8801 doesn't have a clear specification about the actuator speed on the datasheet. In order to explore the upper rate, a couple of tests have been run with sufficient vertical indentation clearance. Although, the results show that an overshoot had been observed when the dynamic indentation velocity is set above 70mm/sec, this servohydraulic system 8801 has an excellent accuracy when the dynamic indentation velocity is below 70 mm/sec. Thus, the dynamic indentation test utilizing this testing apparatus would be used to verify the dynamic indentation model and simulation results.

Figure 23. Instron servohydraulic system 8801

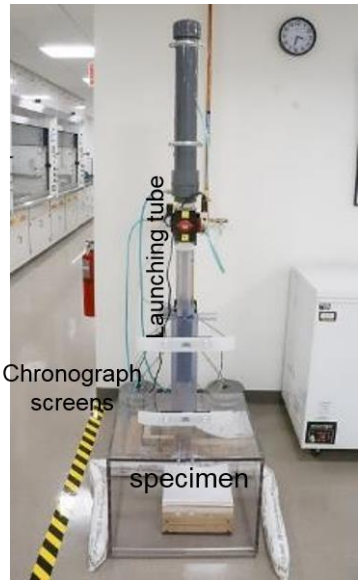

Figure 24. The testing rig, gas gun to launch the lab made ice-ball projectile

The impact tests are performed with a gas-gun apparatus at GAF Materials Corporation. Figure 24 shows the gas-gun apparatus. During the test, the projectile is inserted into an acceleration tube. Depending on the impact velocity, the pressure of pressurized helium-gas can be adjusted to a specific level. While reaching a specific level of pressure, a valve for pressurized helium-gas opened to accelerating the projectile through the acceleration tube to impact on the specimen. The spherical projectile can accelerate to the same velocity level as hail. The specimen is fully supported by the wood block on the ground. A surrounding chamber is assembled to covering the whole testing apparatus for the protective purpose. The specimen should be aligned so that impact events will occur at least 100 *mm* from the edge to avoid the effects that the edges of the structure would have. A spherical ice ball projectile of 25.4 *mm* radius and weighting 60 g is propelled by pressurized gas released from the

launching tube. The most common impact geometry is a spherical impactor, 2" (5.08cm) diameter ice-ball. The impact velocity is measured using a Chronograph. Impact velocity is controlled by adjusting the gas pressure in the cylinder. The physical and mechanical properties of each component are listed in the Appendices A.

Figure 25. How the impact force measurement system works

A high-speed dynamic load cell can be used for measuring the reaction force during the impact events in order to collect data in the future. The impact force sensor manufactured by Loadstar Sensors. The load cell capacity is 2,200lbs which is sufficient for the impact peak load with the gas gun. The testing samples were place on top of the platform and it dynamically measure the force as a function of time. This can be very helpful to verify the finite element simulation and for quickly comparing the energy absorbed for different layered composite structures. It has a high speed USB interface DI-1000UHS-1K to transfer the data to the laptop. According the modal analysis, the natural frequency of the compliant layered composite structure is under 150Hz, therefore a data capture rate with 1KHz should capture sufficient data points, but the higher the capture rate the better. The benefit from this solution is that it can easily be sued for many different kinds of transient loading situations, not just soft covered

structures, but solar cell materials, asphalt, etc. By sorting the plots generated by the data, the desired values of the first impact can be obtained.

Several different materials can be used for the experiments. For the matrix material, GAF Materials Corporation has provided sample sheets of the thermoplastic Polyolefin (TPO) and PVC membrane that are used in commercial roofing applications. A fiber scrim reinforcement is adhered between two layers of TPO or PVC together by a co-extrusion technique. A polyisocyanurate matrix can be examined in bonding with different layer of materials noted above. Different configurations will be used, from simple composite sandwich panels to more complex sandwich panels with multiple layers of TPO/PVC composite. With successful characterization of the materials properties, the dynamic indentation and low velocity impact tests with the spherical indenter were performed to investigate the failure mode and mechanism of the material constituents.

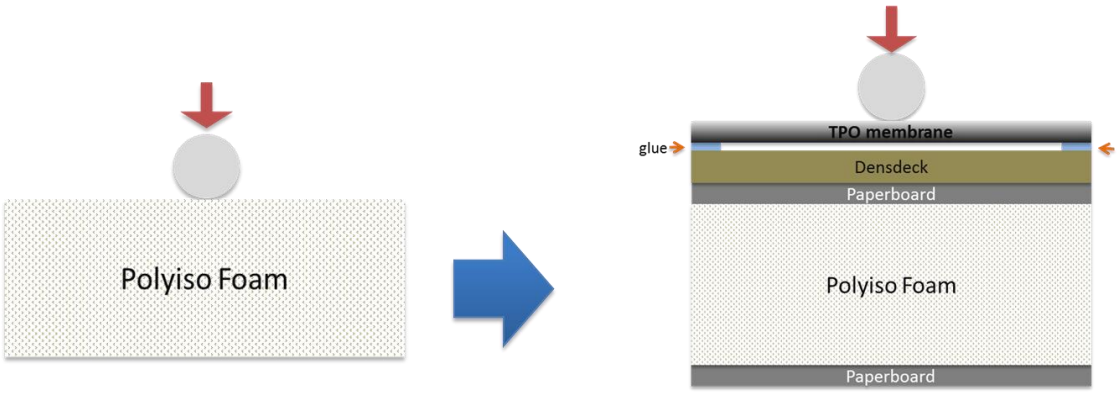

Figure 26. Different configurations from single material structure to complex sandwich composites

Chapter 3. Low Velocity Impact Tests of Layered Foam Composites Panels

In this chapter, effects and failure modes of the constituents of the layered composite panel will be discussion. The impact evaluations are necessary after the impact tests have been performed. In some cases, the material properties can be evaluated by the tests to improve the prediction of the model, e.g. comparing collected data to previous experiments or predictions. A non-invasive examination is performing a close visual inspection to the test specimens. It's usually the first and simplest evaluation method by measuring the permanent deformation and shape of the damaged spot. Any visible failures which including delamination, cracking, buckling and breakage are noted. In some instances, a destructive evaluation method is required to better investigate the internal physical failure modes or failure mechanisms. The numerical solution of the impact event, which will be discussed in next chapter, can be an efficient tool to investigate the failure mechanisms

3.1. Strain-Rate Dependency Investigation

During the impact events of interest in this study, the impact velocity has a range between 1m/s to 100m/s. this represents a loading rate that is significantly higher than the loading rates used to obtain the base material properties. The displacement rates in the experimental measurements were usually less than 70 mm/s. The impact velocity of

a projectile will affect the performance of the layered foam composite panels. However, the mechanisms associated with the different velocities needs to be quantified. Shim, *et al.* [1] has described the differences observed between low and high velocity impact. With low velocity impact, the yarns, which play the important role to carry the load, do not fail during the initial stress rise. Therefore, the deflection and shrinkage of the fabric yarns has time to propagate to the edges of the panel, which allows the fabric yarns to absorb more energy. At the high velocity impact event, the damage is localized and the fabric yarns fail before the stretching or shrinkage occur. For the indentation test, the contact area was increasing as the indenter driving into the substrate. The material right underneath the indenter was in the densification zone. At the outer edge of the contact area, the specimens were ruptured by tensile load. The rupture of outer bound of the contact foam area limited the consolidation of the foam and the strain hardening.

Usually the material has significantly different mechanical response when loaded at quasi-static condition, low velocity impact, or ballistic impact, respectively. In order to characterize the performance of a composite under varied loading rate, a variety of tests need to be performed. The first important testing procedures require dividing the condition of the projectile impact, into quasi-static, low-velocity and high-velocity impact conditions. At low-velocity impact event, the strain rate has a range $10^{-1}\ m/s$ to $10^{2}\ m/s$, which results in the stress to the local region of impact. At high-velocity impact event, the strain rate can be above $10^{3}\ m/s$, which will introduce the wave propagation and vibration. At quasi-static stage, the loading rate usually less than $10^{-4}\ m/s$, which can cause the shrinkage of outreach fiber toward the point of impact.

In the indentation verification experiments on the composite system, the tests were conducted at different velocities varying from 0.25 mm/s to 70 mm/s in order to compare the data at a variety of displacement rate and estimate the loading rate effect on the layered composite system. A typical roofing system is stacked in order of hyperplasic TPO composite, Densdeck, and Polyisocyanurate insulation foam which has been shown in Fig. 30. A 25.4 mm ×25.4mm ×58.3mm test specimen was used for this indentation tests. Spherical steel indenters with 16mm diameters were used. The bottom of the square specimen used in the indentation tests was fully supported by a steel plate. An Instron 8801 servohydraulic fatigue testing system was used to perform the indentation tests at velocities up to 70 mm/s. the "dynamic" indentation tests were used to validate the dynamic indentation finite element results. Figure 7 shows the force vs. deflection measurements obtained from the high-speed indentation tests. Neglecting the data from the lowest loading rate at 1.0 mm/s, in Figure 7, the roofing system appears to have an almost constant mechanical response to the dynamic indentation for loading rate varied over almost one order of magnitude. In order to predict the complicated impact behavior associated with the layered roofing system model, the mechanical response from the dynamic indentation results were deemed to be adequate for finite simulations at even higher velocities. Though it's expected that the rate sensitivity of the various material properties will not change significantly within the velocity range of

interest, i.e. between 0.1 m/s to 40 m/s, this assumption should be verified through addition high speed testing.

A series of tests were performed to justify the strain rate effects to the material constituents. Figure 27 shows the bulk response from dynamic indentation test to single Polyisocyanurate foam board at varied strain rate. In Figure 28, there is a combination of densdeck and Polyiso foam with dynamic indentation test with a 5/8inch indenter. Figure 29 shows the bulk response from a layered composite panel, which is a stack of TPO composite, high-density Polyisocyanurate foam board, and low-density Polyisocyanurate foam. The layered composite panel shown in Figure 30 has densdeck instead of high-density Polyisocyanurate foam board.

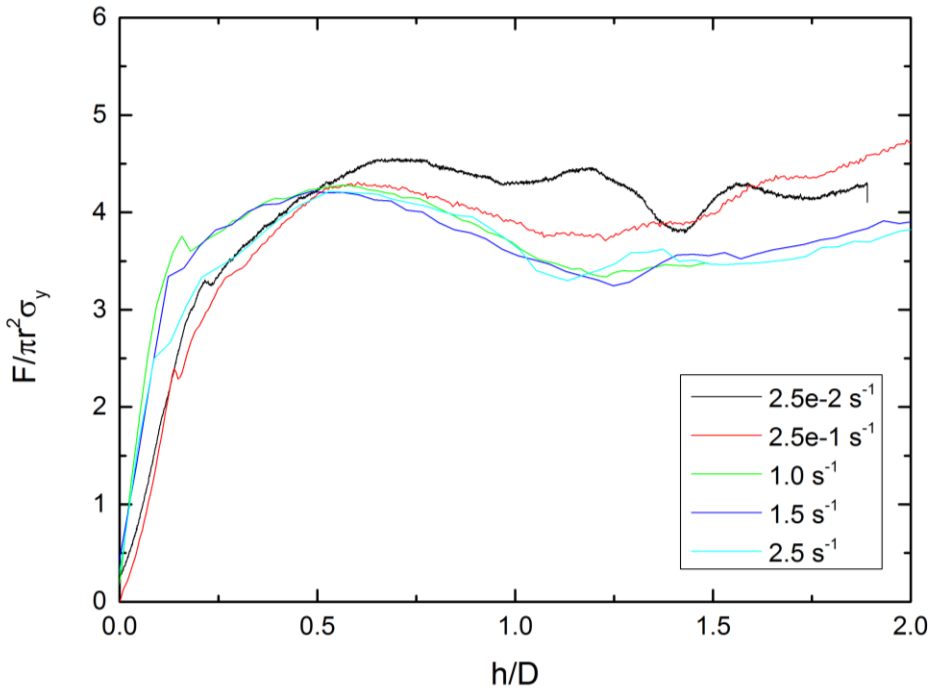

Figure 27. Dynamic indentation test to Polyisocyanurate foam with 5/8" spherical indenter

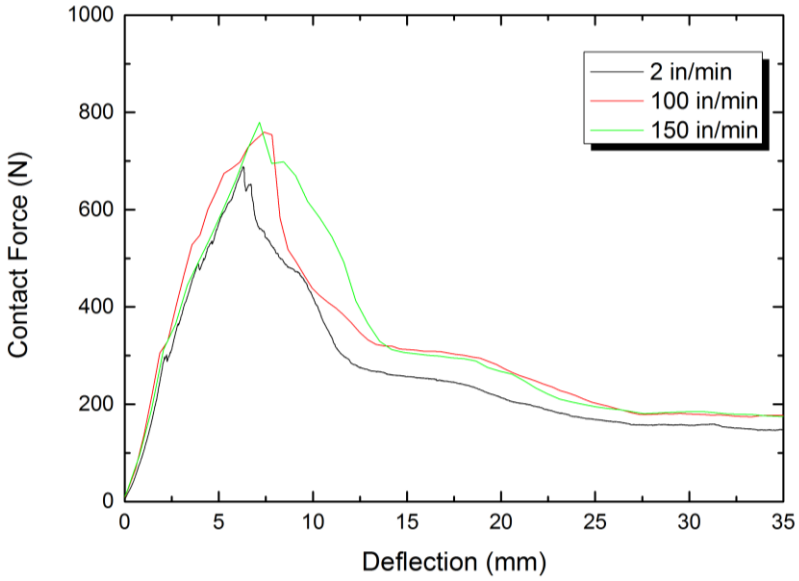

Figure 28. Dynamic indentation test to Densdeck with ISO foam substrate (5/8" indenter)

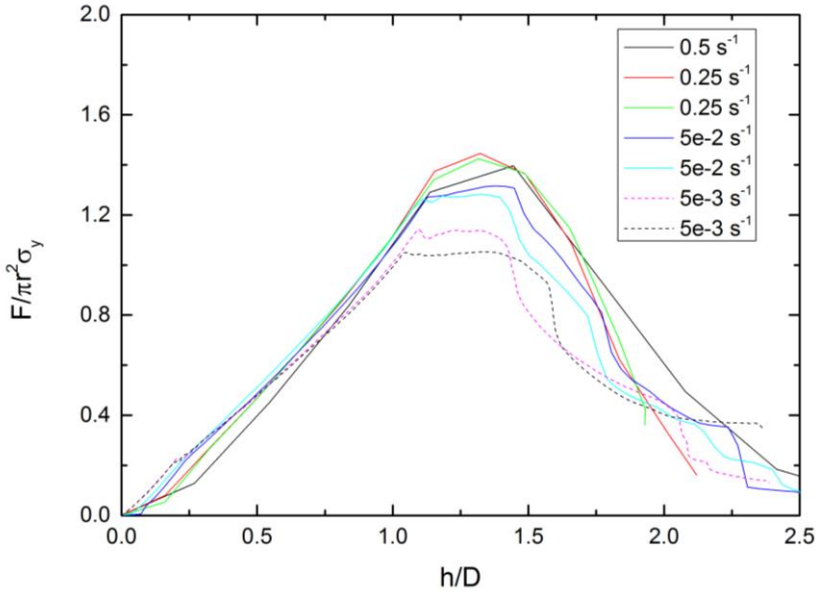

Figure 29. Dynamic indentation test to TPO layered composite panel with 5/8" Indenter

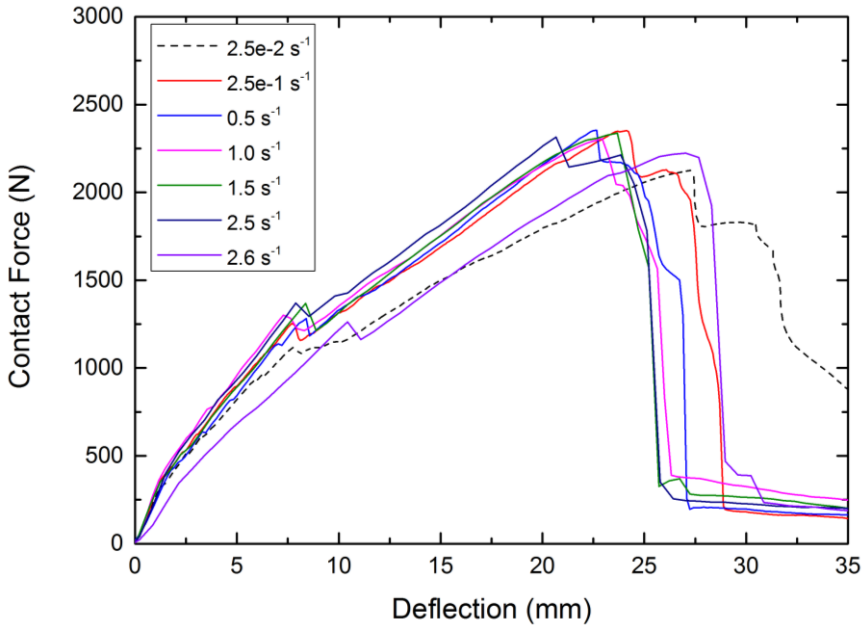

Figure 30. Dynamic indentation test to TPO layered composite panel with 5/8" Indenter

3.2. Effects of Composite Constituents

3.2.1. Effect of Fibers

The impact into a single fiber will be described here. The high-strength, high-modulus fibers, bundled into yarns, has been able to develop the impact resistant fabrics and compliant laminates. When impacted, the stress on the yarns has a sharp increase, and the value of the stress depends on the impact velocity. When the impact velocity is sufficiently low, the stress increase is not high enough to rupture the fibers, therefore allows the transverse deflection and yarn extension propagate, resulting in the absorption of energy by the fibers [17]. Fibers possessing high-tensile strength and large failure strains can absorb a big amount of energy. Lee, *et al.* [2] correlated the number of yarns broken to the levels of impact energy absorbed and stated that the fiber straining

is the primary mechanism of the energy absorption in the penetration failure of ballistic textiles. Roylance, *et al*. [8] have state that the response of the fabrics cannot be determined from the properties individually, however the fabric geometry combined with material properties produce a structural response during the impact event.

When impact event occurs, the yarn experiences a sudden stress increases. The magnitude of the stress is correlated with the impact velocity. At a certain low-velocity, the initial stress is not enough to rupture the fiber. Thus it allows the fiber to deflected and extended resulting in the absorption of energy by fiber [18]. Numerical studies by Roylance [19] have shown that the majority of the kinetic energy of the projectile is transferred to the principal yarns as strain and kinetic energy. Also, high-tensile strength fibers and large failure strains can absorb significant impact energy. Cunniff and other researcher noted that the energy absorbed above V50 – the velocity at which 50% of the projectiles perforate the target – is smaller, since it reduces fiber straining by limiting the time for transverse deflection to propagate [1,8]. By distributing the energy to a wider area, the materials with high-wave velocities can propagate stresses and strains quickly to neighboring fibers, thus involving more material during the impact event [19].

With quasi-static perforation of this study, a large region of stretching is produced. Figure 31 shows the deformed location. When a projectile strikes a layer of fabric, the fabric deflects transversely, resulting in the increase of the spaces between the yarns. If the projectile is relatively small comparing with the size or thickness of yarns, the projectile has a chance to slip through the opening by pushing yarns aside instead of

stretch the yarns to their breaking point. Holes generated in TPO membrane are always smaller than the projectile diameter, which indicating that the projectile perforated the TPO membrane with fiber reinforcement by breaking a few fiber yarns and slipping through the small opening.

One thing worth to note here is that the failure tip of the fabric yarn is located at the outer bound of the contact area rather than at the center spot. It is highly possible that the center spot is sustain much higher compressive load during the impact deformation process than the outer bound of the contact area. At the center spot, the compression loading reinforces the local region material which leads to a higher ultimate strength. But for the material at the outer bound, it suffers from high distortion and tension load, which results in an early breakage failure. More figures of samples failure are in the Appendices section.

The geometry shape of the projectile can be another shape other than spherical ball. Thus, a cylinder rod with flat head in welded to the thread in Figure 32 can produce a severe stress concentration during the penetration.

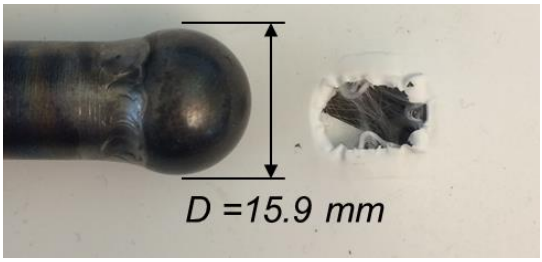

Figure 31. Comparison of the size of indenter with the opening after perforation

Figure 32. Indenter with flat head D = 9.5mm (left) with spherical head D = 15.9mm (right)

3.2.2. Effect of Polymeric Matrix

For the polymeric matrix, the level of ductility and hardness are the main issues that can be studied. Morais, *et al.* [21] examined the impact performance based on the thickness of the laminates which showed a relationship to the amount of incident impact energy. Basically, the thicker the polymeric matrix is, the higher load it can sustain. This thickness effect has been found during the test of thermoplastic polyolefin (TPO) membranes with the thickness of 45mil, and 60mil. These membranes all fabric scrim reinforced and the 60mil membrane sustains the higher load capability resulting in the higher impact energy absorption.

When the textile architecture is used as a composite reinforcement, a polymeric material fills in the spaces, restricting the sliding movement of textile. If the matrix material is a rigid one, such as thermoplastic polyolefin (TPO), the structure gains stiffness at large deformation. The polymeric matrix serves as a medium to bind the fibers together as well as to evenly distribute the load to the fibers. Another purpose of

the matrix is to protect the fiber yarn from damage due to abrasion or chemical erosions, otherwise, the fiber would be compromised. The introduction of a polymeric matrix can minimize the actual physical lateral motion of the yarns. Walsh, *et al*. [20] and Lee, *et al.* [2] have experimentally observed the matrix restricting the lateral motion of the yarns. This restraint forces the projectile to engage and involve more yarns in the composite than the corresponding fabric, resulting in more energy being absorbed by the composite.

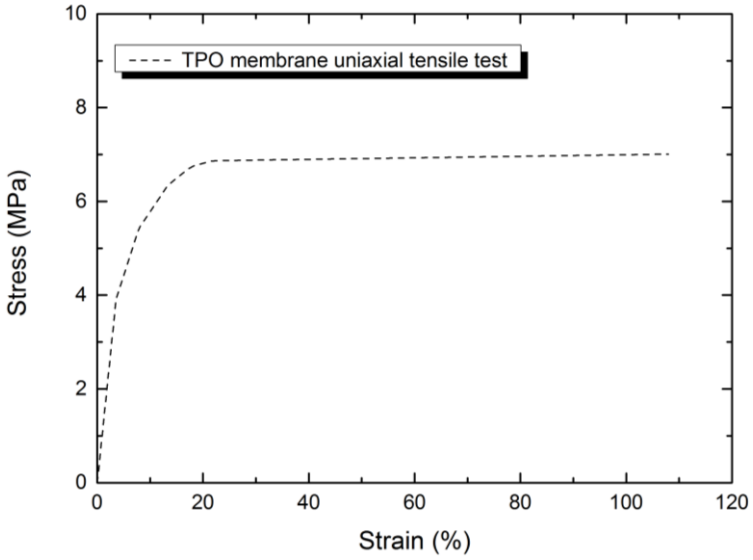

Figure 33. Stress vs. Strain curve of TPO membrane

As the yarn pull-out is responsible for the energy absorbed during the impact event, the frictional interaction between yarns and polymeric matrix play a role in the absorption of the energy during the impact event. The yarn-yarn friction has also been noted in the numerical study on impact performance [22]. Figure 20 shows a transparent

thermoplastic polyolefin (TPO) membrane sample with fabric scrim reinforcement. This transparent Polymer/scrim sheet was produced by the GAF research Lab. This sample has a transparent sheet of polymer extruded onto it, so the geometry was exposed. The damage of the yarn scrim could be observed without further destructive analysis.

Figure 34. Transparent TPO membrane with fabric scrim reinforcement

During the quasi-static indentation tests to the layered TPO membrane structure, the fabric yarns, which are underneath the projected area, were suffering severe stretch and slippage. A perfect bonding or clamping was difficult to achieve in this structure application. However, this slippage feature distinguishes quasi-static indentation ($V_0 < 0.5mm \cdot s^{-1}$) from low velocity impact. Figure 35 exhibits the fiber yarns slippage after the quasi-static dynamic indentation test to the layer foam composite materials. The thermoplastic polyolefin (TPO) membrane with fiber reinforcement was adhered to the substrate. During the quasi-static indentation process, the stress load is distributed to the fiber yarns and causing the stretching and delamination at the yarn-polymer interface. There is no obvious sign of fiber yarn slippage during the low velocity impact. It implies that the delamination growth rate is correlated with the strain rate during the deformation.

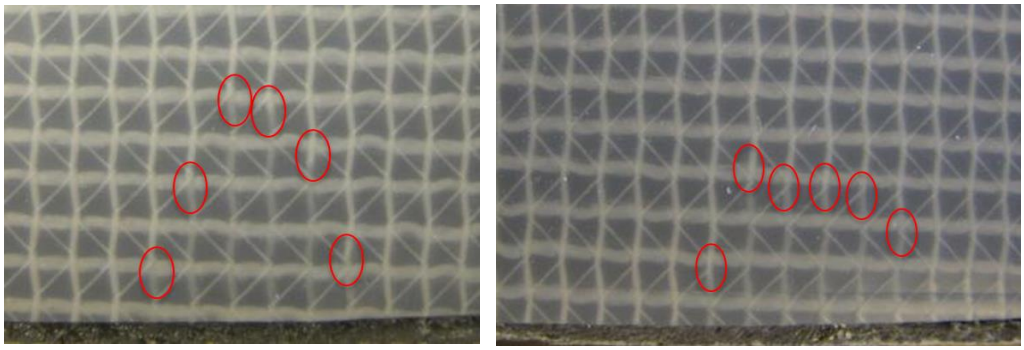

Figure 35. Fabric yarn slippage, red circle shows the tip of the pulled yarns

3.2.3. Effect of Low Modulus Foam

The closed-cell foam material represents a substrate that significantly contributes to the impact absorption capability of the entire layered composite with its unique cell structure. In this study, Polyisocyanurate foam was used as the low modulus soft backing to the layered composite panels. The Polyisocyanurate also referred to as polyiso or ISO, is a thermoset plastic typically produced as a foam and used as rigid thermal insulation. Its mechanical parameters and failure modes were characterized in the lab and would be discussed in this section.

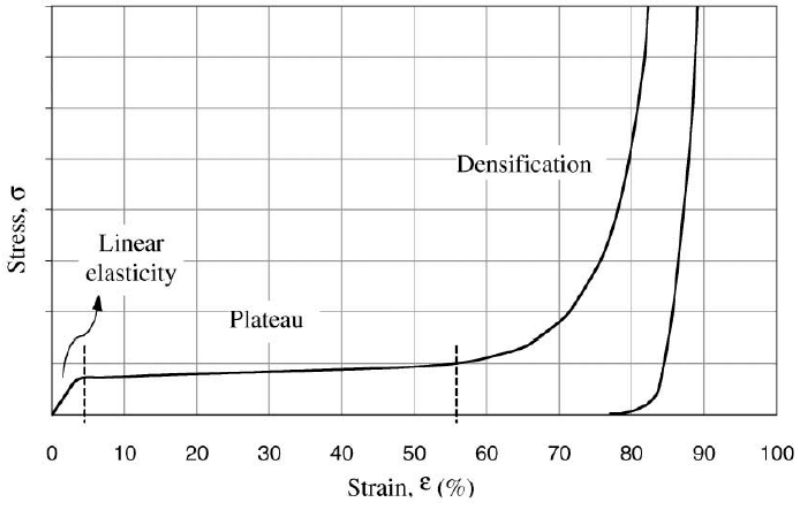

Figure 36. Typical foam stress-strain curve (quasi-static)

As small strains less than 5% in compression, the behavior is linear elastic. As the load increases, the foam cells begin to collapse depending on the mechanical properties of the cell walls. Cell distortions occur at multiple cells along a band. The cells do not collapse because the cells contain curved or wiggled membranes during distortion. The plastic buckling and bending of individual membranes cause both elastic distortion and rotation. Collapse progresses at roughly constant load, indicating a stress plateau, until the opposing walls in the cells touch the next wall along the loading axis, where densification causes the stress to increase steeply. In densification stage, the collapse across the entire loaded section, and hardens its region, leading the collapse process to repeat in different regions. In cell-level distortions and rotations, within each band of enhanced deformation, some membranes have plastic buckling and bending while others remain elastic.

In Stage I, there is no evidence cell distortions (from X-ray images), but the slope of the loading curve is lower than the unloading modulus. As small strains less than 5%, the behavior is linear elastic. As the load increases, the foam cells begin to collapse in stage II depending on the mechanical properties of the cell walls. Cell distortions occur at multiple cells along a band. The distortions include phenomena based on geometric and material nonlinearities: (i) plastic buckling of cell membranes followed by localized membrane plasticity; (ii) bending of at least one membrane. Although these inelastic mechanisms exist, the cells do not collapse because the cells contain curved or wiggled membranes during distortion. The plastic buckling and bending of individual membranes cause both elastic distortion and rotation. If the neighboring cells have similar strength, the stress will be sufficient to redistribute and deform the neighboring cells, normal to the loading axis. But because an elastic enclave is formed, it provides a hardening mechanism to limit the deformation within discrete bands, instead of entire region. Collapse progresses at roughly constant load, indicating a stress plateau, until the opposing walls in the cells touch the next cell along the loading axis, where densification causes the stress to increase steeply.

Also in stage III, one of the bands that generated in this stage has complete plastic collapse. This process spreads the collapse across the entire loaded section, probably because of the transfer of the stored energy into the collapse band [23]. The collapsed band does not propagate normal to its plane. Instead, it hardens its region, leading the collapse process to repeat in different regions, each time coinciding with a macroscopic stress oscillation.

The measurements and observations of cell-level distortions and rotations have established several factors that govern the inelastic response of commercial, closed cell metal foams. Within each band of enhanced deformation, some membranes experience plastic buckling and bending while others remain elastic.

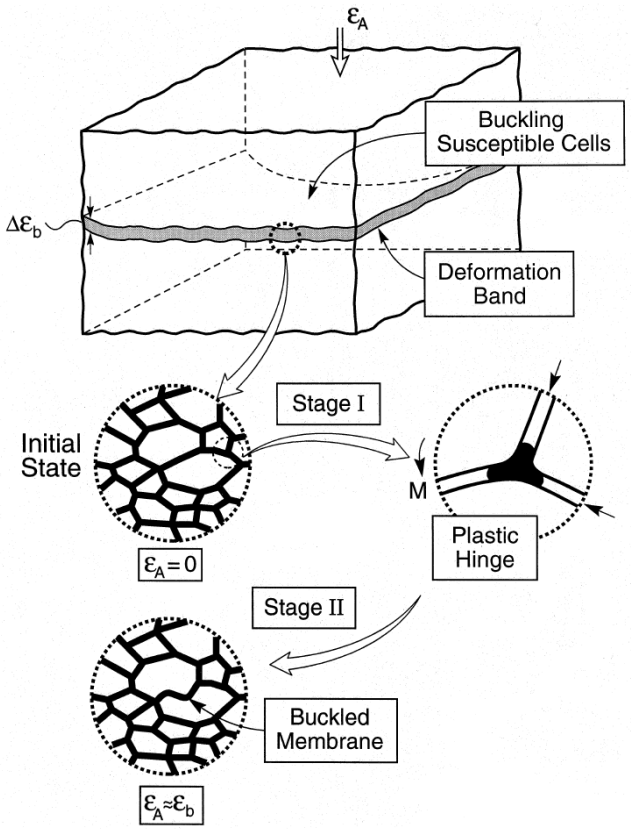

Figure 37. A schematic indicating the phenomena that occur during the three stages of plastic deformation in a cellular Al Alloy subject to compression [23]

Due to the closed-cell nature of Polyisocyanurate, it could be highly distorted. The axial tensile load is more likely to rapture the closed-cell structure during deformation. Initially from the tensile stress vs. strain curve in Figure 19, the foam exhibited elastic behavior which is nominally linear due to the cellular wall elastic elongation. The cell

would rupture after passing its ultimate tensile strength and initiate the propagation of the crack and failure to the whole structure [24]. The overall tensile fracture strength can be used as the cut-off value in the failure criteria of the crushable foam model which would be introduced in Chapter 4.2.3.

Figure 38 shows the contact force vs. deflection non-linear response during the process of indentation tests. The indentation tests with a 1-inch diameter spherical indenter was performed at an array spots and stopped at a series of maximum distance of penetration. It provided an opportunity to cross-section the specimens for post-indentation analysis in order to exanimate the failure mode and crack propagation occurring from the internal of the foam materials. The first peak load noted at round 4 mm displacement is caused by the crack failure of the paperboard on the contact surface of the foam. Then as the indenter keep driven into the substrate, the deformed region increases with the sub closed-cell foam structure buckling, which corresponding to the plateau stage in compression load. Figure 38 shows the cross-sections of the Polyisocyanurate foam as the incremental penetration tests with spherical indenter.

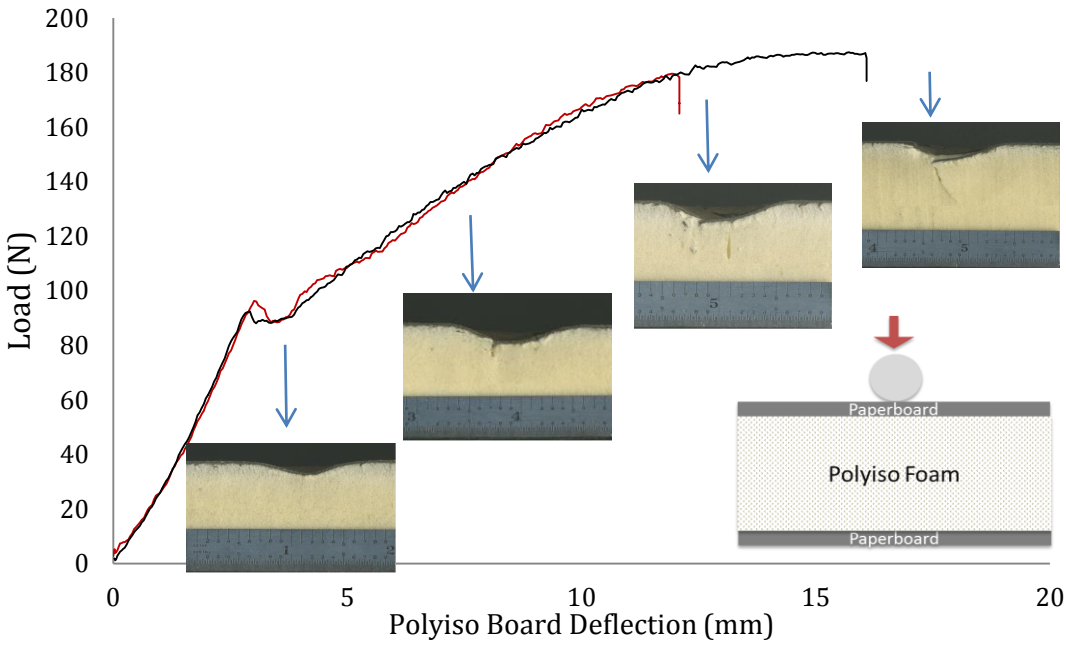

Figure 38. Force vs. deflection curve of Polyisocyanurate foam board

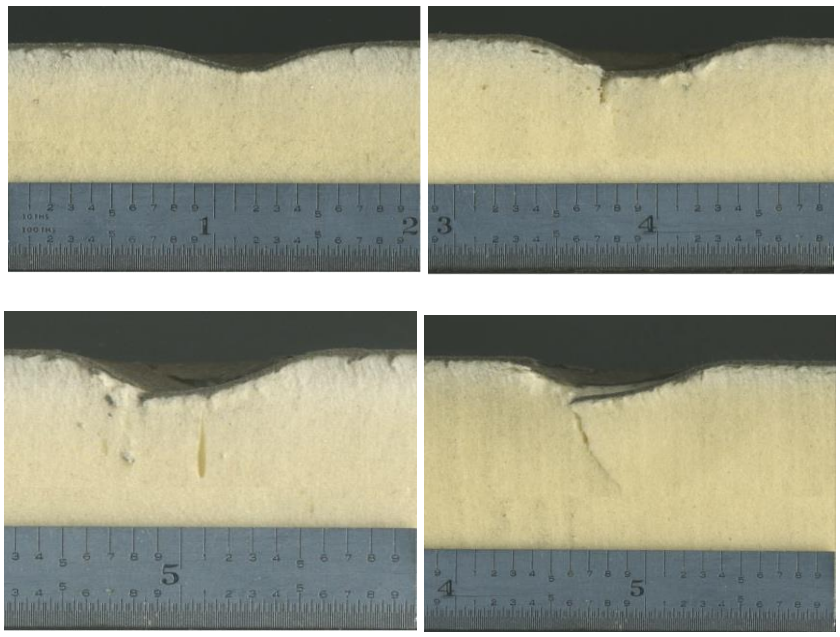

Figure 39. Cross-section to the Polyisocyanurate foam in progressing stage of indentation tests.

3.2.4. Effect of Contact and Boundary Condition of the Layered Composites

The contact of two bodies is a fundamental problem in the mechanical structure, which has a wide range of applications. The contact behavior plays an important role, both directly and indirectly on the impact performance of the layered foam composite panel. At the section of 3.2.2, the yarn pull-out is directly responsible for absorbing energy during an impact event. Applying the matrix to the fiber yarn will restrict the mobility of the yarn, therefore the projectile will engage more fiber yarns and break them, resulting in greater energy absorption due to the higher friction. Many researchers have studied the importance of the contact behavior for impact event. Kim, *et al*. [26] investigated how the surface treatments affect the overall properties of the matrix and reinforcing fibers. The study found that a stronger interface will absorb lower energy with a brittle fracture mode, while a weaker interface will deal with higher energy absorption.

An approach to the interface effects was the comparison between the adhered contact against sliding & lifting contact in Marco-scale. In the experimental indentation test, the TPO composites had two types of contact manner with the low-modulus backing Polyisocyanurate foam, fully adhered, and contact but allows sliding and lifting. In the experimental tests, the TPO composites either adhered to the Polyisocyanurate foam which is called as fully adhered contact, or laid on top of the foam which is called as sliding and lifting contact. A 1-inch diameter spherical indenter was used to penetrate

the layered structure. The deflection and contact forces were measured for further comparison. The force vs. deformation curves of fully adhered vs. sliding & lifting, which are shown in Figure 39, are initially matching with each other until the TPO membrane starts to lift up. In the case of sliding & lifting contact, the fiber yarns are not carrying as much load as fully adhered one does. The Marco-scale sliding & lifting behavior will cause a less brittle fracture mode with relatively low energy absorption capabilities, while a stronger interface will result in a multiple failure mode with higher energy absorption.

Figure 40. Indentation test to layered foam composite panel with sliding & lifting behavior

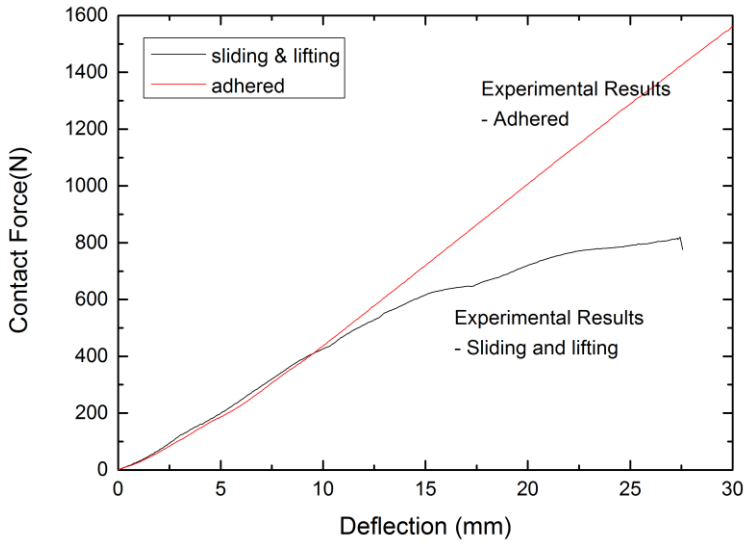

Figure 41. Experimental results: Adhered interface vs. Sliding & lifting interface

In order to evaluate the impact behavior of the layered foam composite panels, the free drop tests were performed. Initially, an *18 mm* diameter spherical ball (24 g) is selected as the impactor. A tape meter is used to measure the maximum rebounce height of the spherical ball then calculate the residual velocity. The spherical ball is free released at a drop height of 2.8m from the targeted foam composite panel, resulting an impact velocity of 7.5m/s and impact kinetic energy of 0.66 J. the layer foam composite panel is in consist of reinforced TPO membrane and high density polyisocyanurate foam board. Two boundary conditions, side-fixed vs. back-fixed have been applied here for contrast. The layered panel is allowed to bend like a beam during the impact event. The back fixed boundary condition has a solid support to back of the layered panel. The maximum rebound height had been captured in Figure by camera to calculate the residual kinetic energy in contrast again the impact kinetic energy. While impact to the

panel with back-fixed boundary condition, the 24g ball contains higher residual kinetic energy, which is shown in the right side of Figure 42. In the left side of Figure 42, the same ball has relatively lower residual kinetic energy after the impact to the panel with side-fixed boundary condition. More energy has been transferred to the system with side-fixed boundary condition than the other one. The impact damage is invisible due to the low impact energy.

Additionally, another free drop impact test has also been performed with a higher impact kinetic energy. A *50 mm* diameter spherical ball (560 g) is selected as the impactor. The spherical ball is free released at a drop height of 1.8m from the targeted foam composite panel, resulting an impact velocity of 6.0m/s and impact kinetic energy of 10 J. The targeted panel has the same layered materials for comparison. The result is shown in Figure 43. While impacting to the panel with side-fixed boundary condition, the 560g ball contains higher residual kinetic energy, which is shown in the left side of Figure 43. In the right side of Figure 43, the same ball has relatively lower residual kinetic energy after the impact to the panel with back-fixed boundary condition. More energy has been transferred to the system with back-fixed boundary condition than the other one. It indicates the high density foam backing had relatively severe damage in the back-fixed boundary condition in contrast with side-fixed one while dealing with high impact energy. In-depth investigation has been done by numerical analysis which will be discussed in Chapter 4.4.

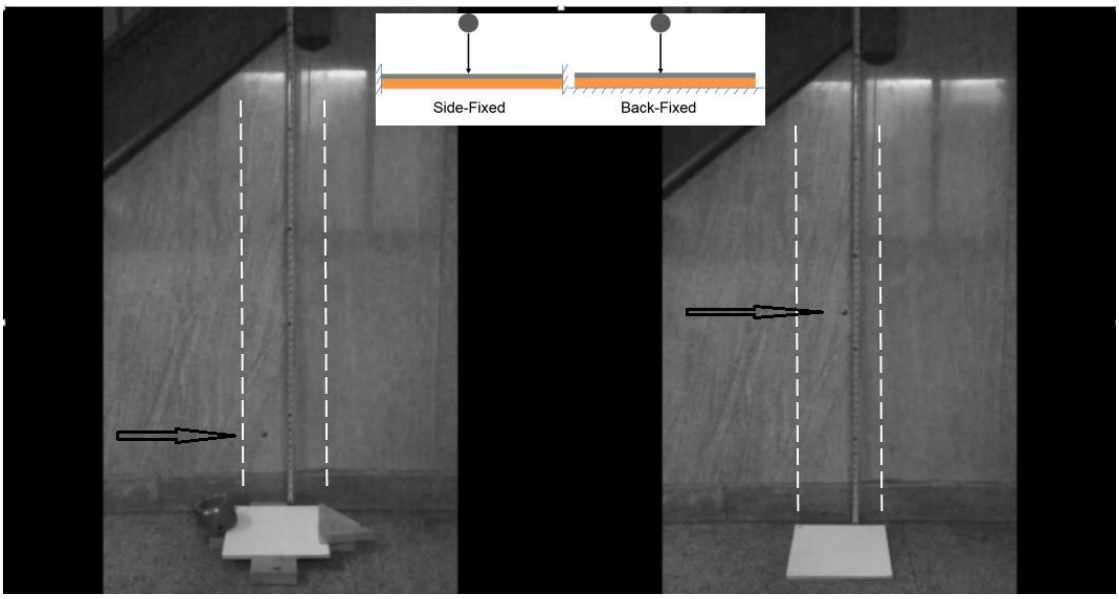

Figure 42. Free drop test of light spherical ball (24g) associated with 7.5 m/s impact velocity, arrows point at the maximum rebounce height of the spherical ball.

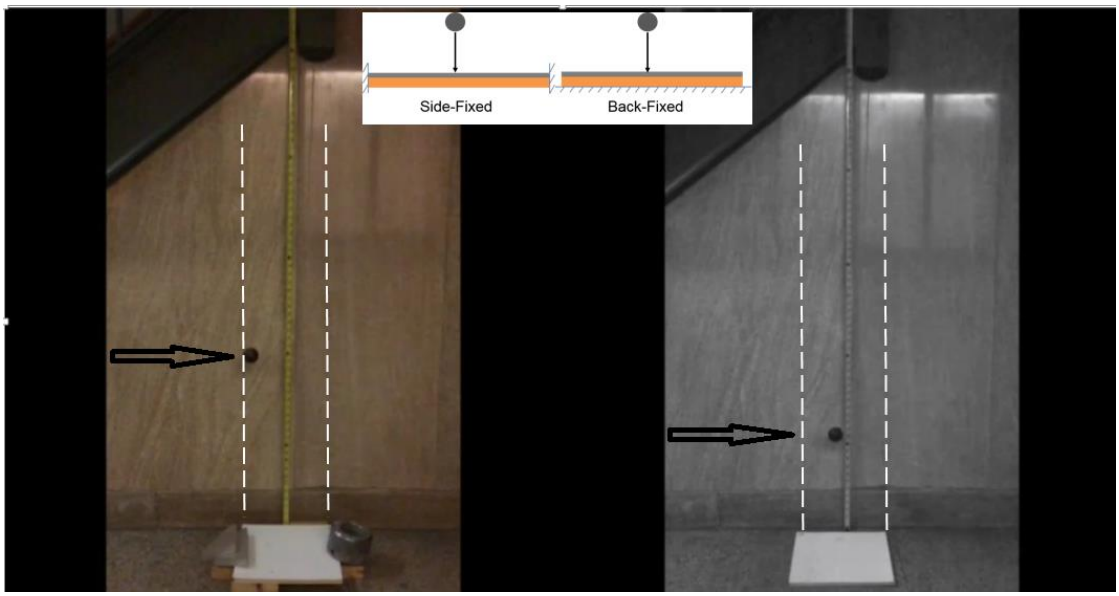

Figure 43. Free drop test of heavy spherical ball (560g) associated with 6 m/s impact velocity, arrows point at the maximum rebounce height of the spherical ball.

3.3. Discussion and Conclusion

There are some major challenges due to the complex contact behavior, non-linear materials, large deformation and impact event. Due to the highly dissimilar material properties of the layered foam composites structure, some interesting comparisons of simulation can be done among the simulation of thickness variation, interface bonding variation, deformation at different strain rate, and composite material selections. Finally, the material failure modes including foam failure behavior, fiber reinforcement indentation crack behavior, and low-modulus backing impact deformation can be simulated by finite element program ANSYS.

Chapter 4. Modeling and Simulations

4.1. Meso-Scale Model

A powerful numerical tools are required for better understanding and utilization of these new material structures. The basic parameters of an impact model are impact velocity, mass, dimensions of the projectile, the mechanical properties of the components, boundary conditions of the model, and appropriate failure criterion for the elements. The element selection will be discussed in this section. An explicit method is recommended to solve the impact behavior of the model. The explicit computational process for this numerical model involves incremental time steps. At each time step, the change of the projectile in displacement is calculated based on its velocity. The rigid projectile forces nodes in direct contact with its surface and cause the interaction between the projectile and the substrate surface. Displacement of the contacting nodes generates stretching and tension in the elements resulting the material component reaches its failure criteria.

Both SOLID164 and SHELL163 are used in explicit dynamic analysis. SOLID164 is typically used to predict the three-dimensional modeling of solid structures. The element is defined by eight nodes having the following degrees of freedom at each node: translations, velocities, and accelerations in the nodal x, y, and z directions. Since the fabric scrim is a thin layer of structure, SHELL163 has been used to predict the structural behavior of the mid surface of the thin layer. SHELL163 is a 4-noded element with both bending and membrane capabilities. The element has 12 degrees of freedom

at each node: translations, accelerations, and velocities in the nodal x, y, and z directions and rotations about the nodal x, y, and z axes. The utilization of SHELL163 element significantly reduced the analysis and optimization costs at the fabric yarns reinforcement modeling portion.

A severe geometric distortion could occur and cause the elements highly distorted during an impact event. It's necessary to have a fine mesh around the critical contact area and explicit analysis is selected for such applications. In order to minimize the analysis computing costs using explicit dynamics, a simple elastic-plastic material model was initially selected for isotropic materials before advancing to more sophisticated models. The material model neglected strain rate dependency, however, it was found to produce adequate experimental/FE correlation for the impact velocity range tested. Comparing the acoustic speed of sound in the materials with the relative low impact velocity, equations of state for the shock propagation of the materials were not used. The projectile is assumed to be a rigid sphere of radius. In the dynamic indentation tests, the projectile was experimentally found to have no permanent deformation.

To further reducing the costs of analysis and optimization, the structure model can be optimized. Considering the actual size 25.4mm diameter of the projectile and the nature of the impact events, the local materials tends to dominate the impact response at the local spot. Therefore, a reduced model size of 100 mm length × 100 mm width was used in the layered composite simulation. If only considering the isotropic material, the modeling can be simplified further by axisymmetry. In this chapter, a quarter

symmetry had been applied because of the orthotropic property of the TPO membrane with fiber reinforcement. It makes sense to start the simulation with a simple model as calibration process and increase the model complexity as necessary to the real layered foam composite structures.

Once the finite element models were set up with good correlation to the proper material data, the impact simulations were performed with a range of impact velocities to generate a numerical curve. The principal erosion strains were enabled in the FE model to mimic the failure of the structure. However, with such failure criterion, the models are mesh sensitive and a mesh insensitive model should be built [27]. For a finer mesh of the model, the computational costs rise.

4.1.1. Thermoplastic Polyolefin Properties/The Mooney-Rivlin Model

In order to correctly evaluate the mechanical behavior of the thermoplastic polyolefin (TPO) material, computational models can be used such as the Mooney-Rivlin model (incompressible elastomers with train up to 200%), the Ogden model (incompressible materials with strain up to 700%), Blatz-Ko model (compressible polyurethane foam rubbers). For incompressible materials, like rubber, the Mooney-Rivlin and the Ogden models are the most adequate [25]. The Mooney-Rivlin parameters can be determined using uniaxial/biaxial tensile tests. For this study, the uniaxial tensile test was applied with an Instron Machine. The specimens were manufactured and tested to determine the tensile stress-strain property of thermoplastic polyolefin.

Payne found that the membrane behave nearly isotropically which is consistent with results found in [28]. The material behaves in a non-linear, elastic manner according to the stress vs. strain curves. It's fit the hyper-elastic material model with isotropic material behavior. With such large deformations, either Orgden or Mooney-Rivlin model is suitable to this flexible polymer material model [29-31].

The Mooney-Rivlin model is based on the strain-energy function. The stress state is determined as the derivative of the strain energy density with respect to the strain components.

$$[S] = \frac{\partial W}{\partial E} \tag{4-1}$$

Where [S] is the second order Piola-Kirchoff stress; [E] is Green-Lagrange deformations and W is the strain energy density [30]. The hyperelastic materials are isotropic and thus the strain energy density W can be expressed as a function of the strain invariants:

The incompressible Mooney-Rivlin model is based on the strain-energy density function:

$$W = C_{10}(\bar{I}_1 - 3) + C_{01}(\bar{I}_2 - 3) \tag{4-2}$$

Where C_1 and C_2 are empirically determined material constants, and I_1 and I_1 are the first and the second invariant of the unimodular component of the left Cauchy-Green deformation tensor.

$$\bar{I}_1 = J^{-2/3} I_1 \tag{4-3}$$

$$\bar{I}_2 = J^{-4/3} I_2 \tag{4-4}$$

$$I_1 = \lambda_1^2 + \lambda_2^2 + \lambda_3^2 \tag{4-5}$$

$$I_2 = \lambda_1^2 \lambda_2^2 + \lambda_2^2 \lambda_3^2 + \lambda_3^2 \lambda_1^2 \tag{4-6}$$

$$J = \det(F) \tag{4-7}$$

Where λ_i are the principle stretches, and F is the deformation gradient. For an incompressible material J = 1.

ANSYS has the built-in function for computation and only requires the stress vs. strain data obtained experimentally. The constants C_{mn} can be solved and produce the plot to fit the experimental data curve. Parameters for Mooney-Rivlin model can be determined using the procedure implemented in the finite element code ANSYS based on the experimental tests. For the model with 5 constants term can be obtained. The following values yielded from the calculations: a10, a01, a11, a02, a20. The obtained value will be used in order to analyze complex thermoplastic Polyolefin structure.

Material Properties were obtained on an Instron Universal testing machine with Measurements Technology Inc. MTI-10K integrated into it. The majority of the tests

were run at 60 mm/min crosshead speed. A Mooney-Rivlin 5-parameter model had been calculated based on this experimental data and then applied to the numerical model to calibrate the parameters and then perform the justification. A testing sample of 6-inch width by 16-inch length by 0.028-inch thickness was held by the customized fixtures. The test area was 6-inch width by 2.5-inch length. A finite element model of this PVC membrane with the same geometry was created. The result of experimental-FE correlation to PVC membrane biaxial tension tests can be seen in Figure 44. There is a good agreement between the experimental data and numerical solutions. The Mooney-Rivlin 5-parameter data then can be used in the simulation of layered foam composite panels.

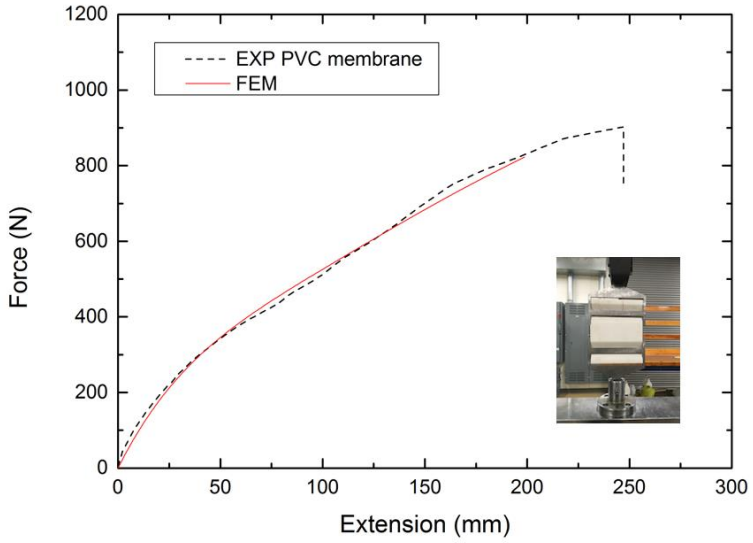

Figure 44. Experimental-FE correlation of PVC membrane with Mooney-Rivlin Model

4.1.2. Numerical Model of Fabric Scrim

The fiber scrim, which is produced by Highland Industries, Inc., is comprised of PET fibers. The fibers can be defined into 3 different types: horizontal fiber, vertical fibers, and the "tie" fibers. The horizontal and vertical fibers create a grid as the way they laid. The "tie" fibers are much thinner than the other two types and tie the joints at the intersection of the other two fibers.

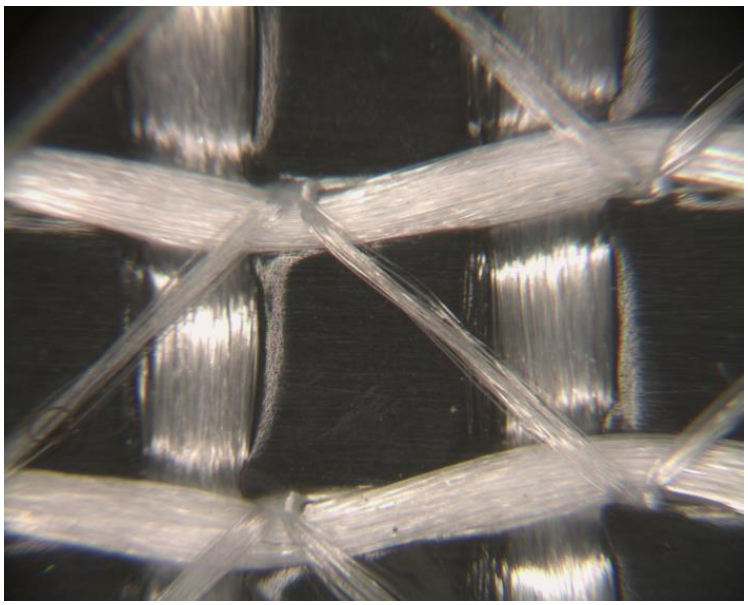

Figure 45. Microscope Image of Fabric Scrim

This Microscope image was taken when the sample was laid on the microscope platform, and was not adhered to any polymer [34]. Thus, a very unstable condition and large variations in material property measurements. Because their discrepancies would not be helpful in creating finite element model, an effective approach was performing the measurement to PVC composites with and without fiber yarn scrim, respectively. Then the materials parameters should be verified by the contact force vs. displacement

data from the puncture tests. Therefore, it's necessary to obtain the material properties for both the fibers and the polymer. The samples of full PVC membrane with scrim reinforcement were examined by its biaxial behavior. The stress vs. strain curve were plot and the basic orthotropic fiber yarn parameters were extrapolated from the curve.

In 3-D modeling, the fiber reinforcement layer is not practical to be modeled as a solid element, since it would involve too many elements and rise the computational cost in a huge amount. In order to solve the global model efficiently, Shell element would be applied for such specific thin layer material. It is also cost demanding to model the fabric scrim by its actual geometry. Shell elements have both degrees of freedom – displacements and rotations. In the finite element modeling, it doesn't recognize the scale of unit selections in either nanometer, micrometer, or kilometer. Therefore, an arbitrary 3-D model of cubic geometry can be created with a 2-D shell plate embedded in the middle of two halves 3-D components as shown in Figure below. The nodes of the 2-D shell plate are bonded to the neighboring nodes on the contacting surface of the 3-D components. A few simple loads were applied to the testing model to verify if the 2-D shell plate has an appropriate contact behavior with the neighboring membrane contact surface. The utilization of SHELL163 element significantly reduced the analysis and optimization costs at the fabric yarns reinforcement modeling portion. Only one element-through-thickness is required with such application.

The $100 \times 100 \times 0.1$ mm fiber reinforcement layer was modelled with an inexpensive elastic material model using a coarse shell element mesh. The material property used were obtained semi-empirical test. It is necessary to prevent overly distorted elements

from causing the time step reduce to a small value and causing the simulation time to a very expensive level. Figure 47 shows a good agreement of Experimental-FE results of PVC membrane with fabric scrim reinforcement under biaxial tension test. This validated membrane model will be applied to the global impact analysis of layered foam composite panel.

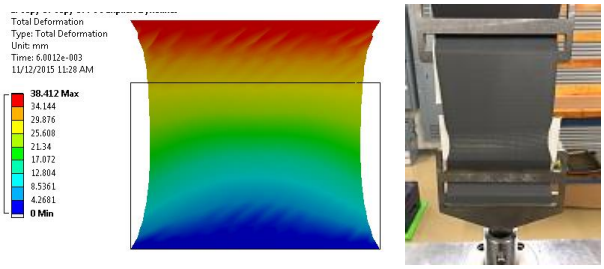

Figure 46. Mooney Rivlin model with embedded shell elements (left), biaxial tension experimental test (right).

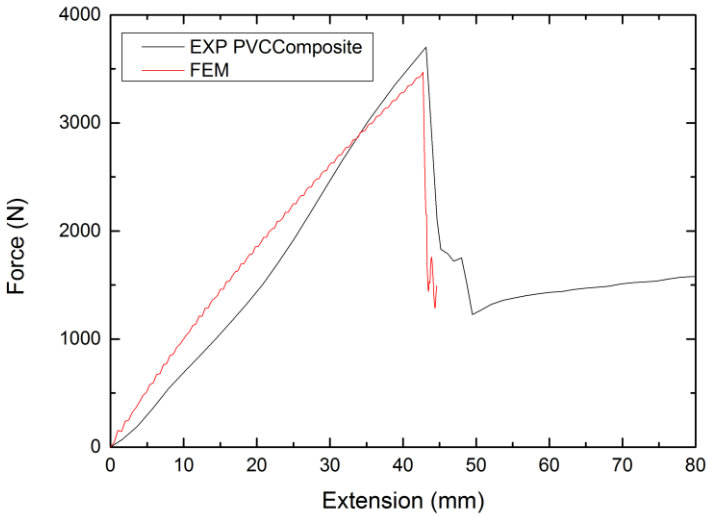

Figure 47. Experimental-FE correlation of PVC membrane with fabric scrim reinforcement biaxial tension result (in black) and numerical result (in red).

4.1.3. Crushable Foam Model

Many researchers had studied this closed-cell foam. A crushable foam model is the most suitable model to capture the feature of the foam material. Finite element method will be used to investigate the large deformation behavior of composites with closed-cell foam, elastomeric matrix and textile fabric reinforcements during an impact event [8].

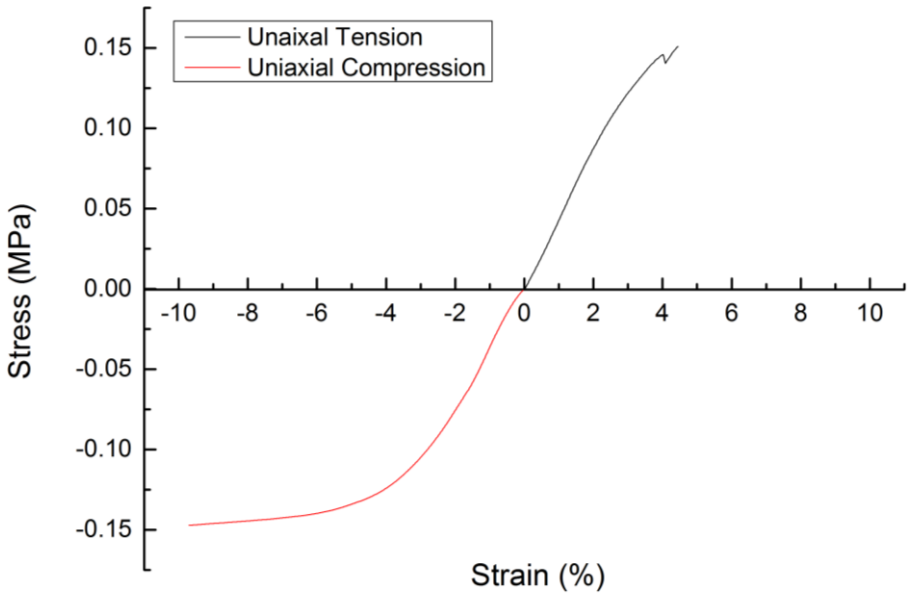

Figure 48. Experimental data of foam stress-strain curve for crushable foam model

The foam specimen in the ultimate tensile strength of the macro-scale foam material was used as the tension cutoff stress for the foam material model in the FEM simulations. Based on this model, an indentation simulation of the Polyisocyanurate foam board was performed to compare the contact force and displacement with the experimental test results. Figure 6 shows the correlated

results. A 25.4 mm steel spherical ball modelled as a rigid indenter, with a specified displacement rate of 0.5mm/s was used to obtain the results shown in Figure 49. Since the foam element can sustain high compressive load without fail, while the tensile stress reach the cut-off value of the crushable foam model, the cell structure in finite element code is eroded resulting the plateau in the contact force vs. deflection curve.

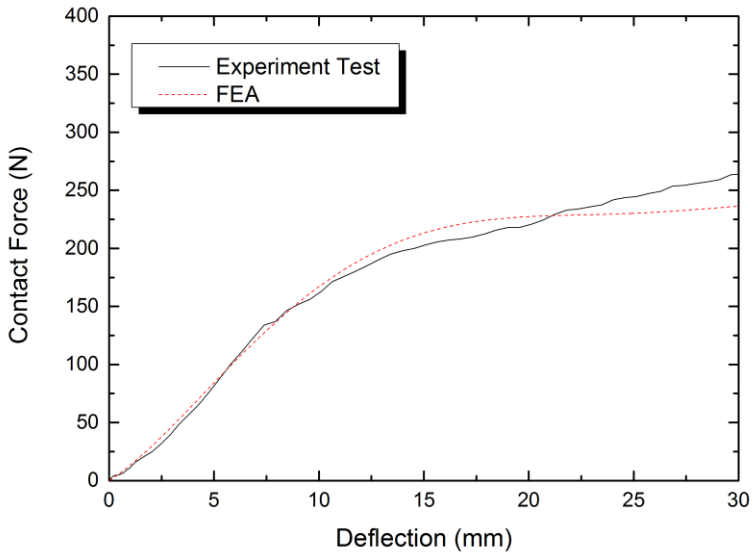

Figure 49. Typical foam model results vs. experimental test data with controlled indentation

4.2. Finite Element Modeling

The finite element method (FEM) is the most popular simulation method to predict the physical behavior of systems and structures of a large number of applications in engineering. Finite element solutions are available for many engineering areas like static, dynamics, fluid flow, heat flow, electromagnetics and coupled filed problems. A

finite element solution is an approximate solution for the engineering problem and the solution need to be evaluated carefully.

By neglecting dynamic effects, a quasi-static energy balance is used. The classical system of finite element equations can be obtained as follows.

$$\{K\}\{u\} = \{F\} \tag{4-8}$$

The solution for the displacement $\{u\}$ is sought with the known stiffness matrix $\{K\}$ and the external force, $\{F\}$. However, this equation is only valid when the displacement is very small and the stiffness matrix can be assumed unchanged during the deformation. For large deformation problems the force term is also dependent on the deformation. Thus, Newton-Raphson, a non-linear solution procedure, is required. The total external force can be divided into small steps for which a solution can be obtained by iterative techniques. After that, each small displacement solution can be added up to find the total displacement at such total force.

$$\{K_t\}\{\Delta u\} = \{F\} - \{R\} \tag{4-9}$$

where K_t is the tangential stiffness matrix, obtained by differentiation of the stiffness matrix with respect to the displacement, F is the incremental external force and R is the internal force vector associated with the incremental displacement Δu. an iterative approach is required to solve the system for Δu.

Once the geometry was established and the material properties were obtained, the full model could start to be built. The scrim reinforcement and the facer would be

modeled using SHELL163 elements. The Polymer layers would be modeled using SOLID164 elements and taking on the 5 parameter Mooney-Rivlin material model.

Some efforts had been applied to ANSYS/explicit finite element model to exanimate the characterization of the system. Both 2D axisymmetric and 3D model were created and there was a good agreement on the model and experimental results. In the FE model, the elements underneath the spherical indenter was removed from the layered composite structure while the tensile stress was reaching to its cut-off value as the indenter driving into the substrate. It was a continuous process with deactivating elements from the system. The finite element model shows that the elements at the center of the contact area started to fail first, which provides the cause of crack propagation in the substrate.

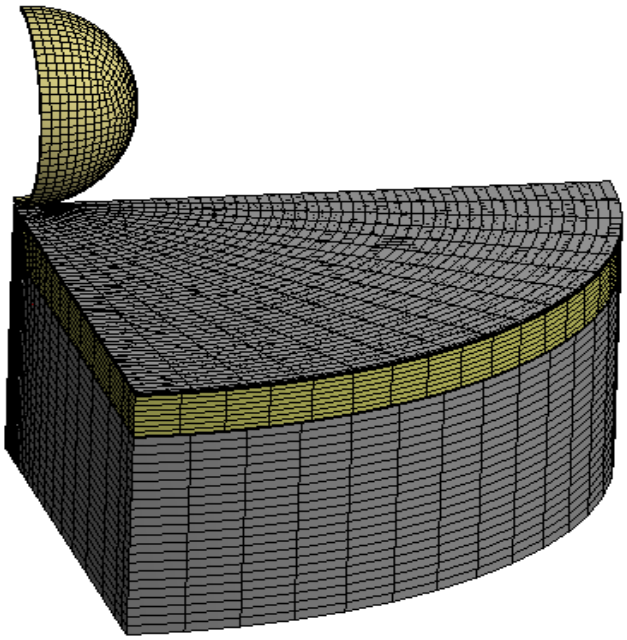

Figure 50. Partial View of 3-D Finite Element Model

However, due to the non-zero frictional coefficient of the contact surfaces of the top layer, it could be simplified as a pre-stressed component in compression. A higher loading was needed to fail this component in tension, because of the state of pre-stressed in compression. Therefore, the actual tensile strength criterion of the component in the layered foam composite system is much higher than its failure criterion characterized from uniaxial tensile test. It provides a possible explanation that the material could sustain higher load from the indentation experiments, comparing with the FE modeling. The model can be constructed from quite simplistic to fairly complex. Several things need to be taken into account when performing FEA for an impact event.

The principal and shear erosion strains were enabled in the FE model to mimic the failure of the structure. With such failure criterion, however, the models are mesh sensitive and a mesh insensitive model should be built [27]. The results from finer mesh would be mesh sensitive due to the strain softening and element deletion, thus a non-local model techniques are required [33]. The failure criteria of the materials has been updated according to the experimental-FE correlation. The indentation test was reproduced in the FE model and correlated with the mechanical behavior of the layered roofing system. A rigid spherical indenter is driven into the TPO/Polyisocyanurate foam substrate with a constant indentation velocity. Figure 52 shows the good agreement in the contact force vs. displacement between the FE model and experimental results. Comparing the contact force in Figure 52, the composite system sustains much higher loads for the same displacement. This shows the effect of the TPO composite membrane on resisting the concentrated indenter load. This indentation tests were conducted for

two types of interface conditions between the TPO membrane and the foam substrate. First where the TPO was bonded to the substrate and second where the TPO membrane was forced to slide and lift from the substrate. When the TPO composite is perfectly adhered to the Polyisocyanurate foam substrate, the composite panel is able to sustain much higher loading forces than the case where sliding and lifting are permitted (see Figure 52). A conclusion is that the adhered system should be able to absorb more impact energy.

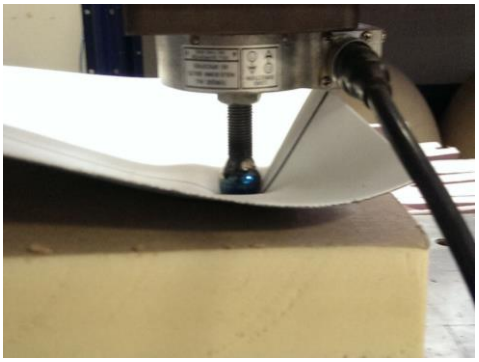

Figure 51. Experimental indentation test to the layered structure with sliding & lifting contact

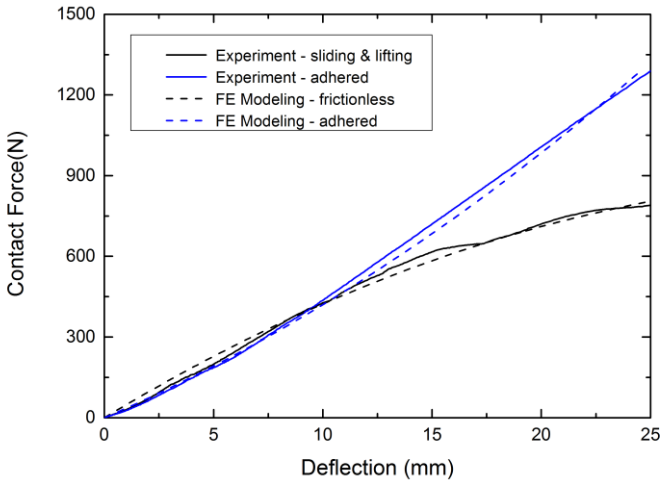

Figure 52. Simulation results in ANSYS Explicit Dynamics

4.3. Roofing System Models

Several polymeric options are available in the roofing membrane applications including ethylene propylene diene monomer (EPDM), polyvinyl chloride (PVC) and thermoplastic polyolefin (TPO). EPDM is an extremely durable synthetic rubber roofing membrane widely used in low-slope buildings in the United States and worldwide. Its two primary ingredients, ethylene and propylene, are derived from oil and natural gas. As a roofing material EPDM has moderate seam strength due to the use of adhesive tapes.

One of the applications of the layered foam composite panels is as roofing system due to its superior weatherability, lightweight and energy absorption capability. As the top layer roofing membrane, it has to be strong enough to withstand loading stresses and flexible enough to transfer the impact energy to the substrate materials such as foam in order to maintain its integrity during the impact event. More specifically, the company's EverGuard TPO (thermoplastic olefin) and PVC were the product of interest. As an example of TPO composites, the material consisted of two layers of TPO co-extruded onto a non-woven sheet of PET (polyethlenne terephthalate) fibers. This material has varied thickness (45, 60 & 80 mil) that adhered on top of a rigid board such as densdeck or HDboard (high density foam coverboard) as shown in Figure 40. The hail impact scenario discussed in a variety of failures, including crack in TPO membrane, crack in densdeck/HDboard, fiber-scrim breakage, and Polyiso insulation foam deformation. The finite element model validated for displacement controlled

indentation tests was used to simulate the more complex TPO roofing system under dynamic hail-stone impact events.

Figure 53. Rigid board: densdeck (left), HDboard (right)

A 50 mm diameter iceball was modeled as a rigid spherical ball with a mass of 60g. The maximum permanent deformation of the TPO roofing system from the simulation directly underneath the impact side can be used to compare with experimental deformation data obtained from gas gun impact tests in the future. The boundary conditions on the bottom of the TPO roofing panel was constrained from moving vertically in the FEM simulations. The simulation results shown in Figure 55 indicate the failure mechanism of the TPO membrane with fabric scrim reinforcement. Foam backing substrate material is omitted in the Figure 55. The damage is localized and the fabric yarns fail before the TPO membrane. For the impact simulation, the contact area was increasing as the indenter driving into the substrate. The material right underneath the indenter was in the densification zone. At the outer edge of the contact area, the specimens were ruptured by tensile load.

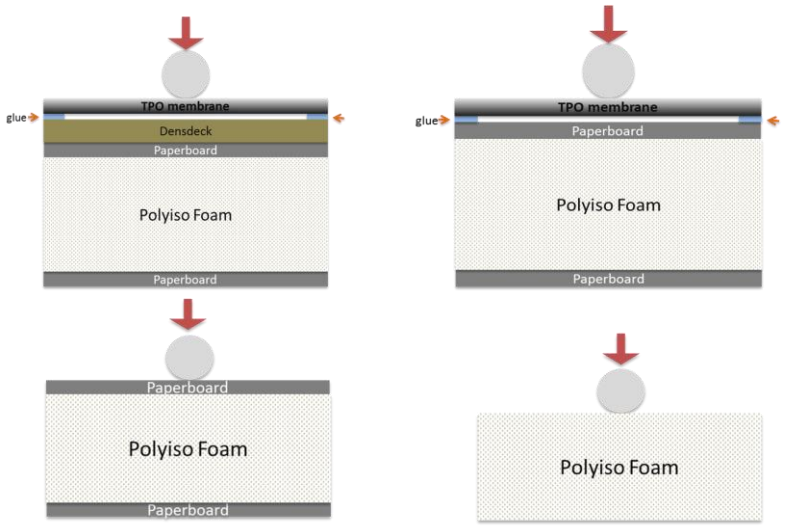

Figure 54. Layered composites panels structures from complex to simple

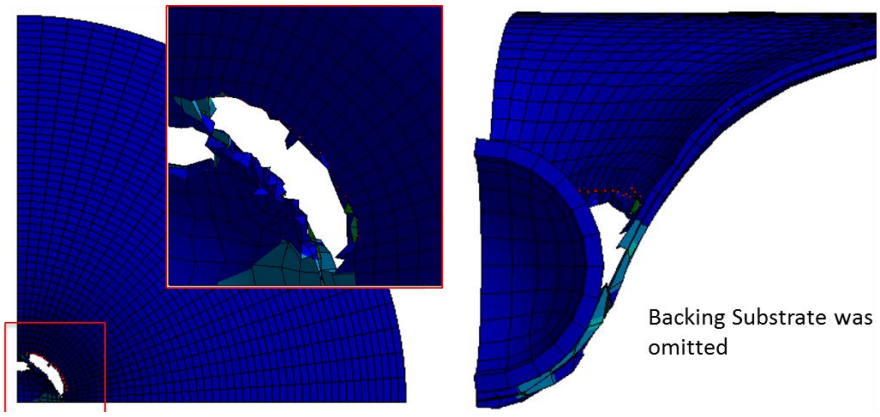

Figure 55. Indentation failure mode of ¼ symmetry model, TPO membrane layer top view (left) and TPO membrane layer side view (right)

Table shows the post-impact simulation results of the membrane causing by impact energy from the 50mm diameter spherical projectile. The membrane conditions are recorded from the numerical solution. The increase of TPO thickness help with the

integrity of the roofing system subjected to hail impact event. However, it is also associated with the manufacturing cost in the engineering applications.

Table 2. Impact Modeling Results of Everguard TPO roofing system

	Everguard TPO								
Thickness (mil)	45			60			80		
Coverboard	1/2" HD								
Iceball	2" Diameter								
Impact Velocity (ft/s)	115	130	145	115	130	145	115	130	145
Kinetic Energy (J)	36.8	48.3	58.7	36.8	48.3	58.7	36.8	48.3	58.7
Condition of membrane									
Critical Impact Energy	~49 J			~ 57 J			~ 71 J		
	Good: No Cracks				Bad: Cracks				

4.4. Boundary Condition Investigation

When testing the layered foam composite panels for impact, the size of the specimen and the means of fixturing condition are important. Developing the shielding concepts to protect critical aircraft components from engine debris, Shockey, *et al.* [16] have performed a number of quasi-static and impact experiments to study the capability of energy absorption at different boundary conditions from barriers. The barriers were made of high-strength polymer fabrics. It was shown that when the specimens were gripped on two edges rather than four edges, more impact energy was absorbed.

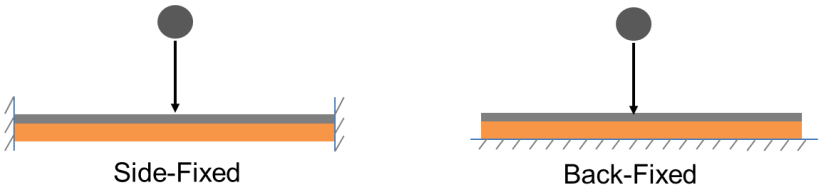

Figure 56. Boundary condition setup in FE modelling

Simulation results in time domain are shown as follows. Figure 57 shows the numerical modeling results of light weight ball (24g & 0.66J Impact Energy) free drop impact to layered TPO/foam panel. Figure 58 shows the results of heavy weight ball (240g & 4.2J Impact Energy). As considering the simulation results of light weight ball associated with low impact energy, the light ball has more residual kinetic energy while the layered panel has back-fixed boundary condition.

On the other hand, in Figure 58 the heavy ball has more residual kinetic energy while the layered panel has side-fixed boundary condition. It indicates a relationship between the impact behavior and boundary conditions. Moreover, the heavy ball which associates with higher impact energy can drive the layered panel further down, resulting the hyperplastic TPO membrane stores the higher strain energy. When rebound, relatively more energy can transfer back to the spherical ball in the side-fixed boundary condition. It results the higher rebound height which is observed in the experimental impact test.

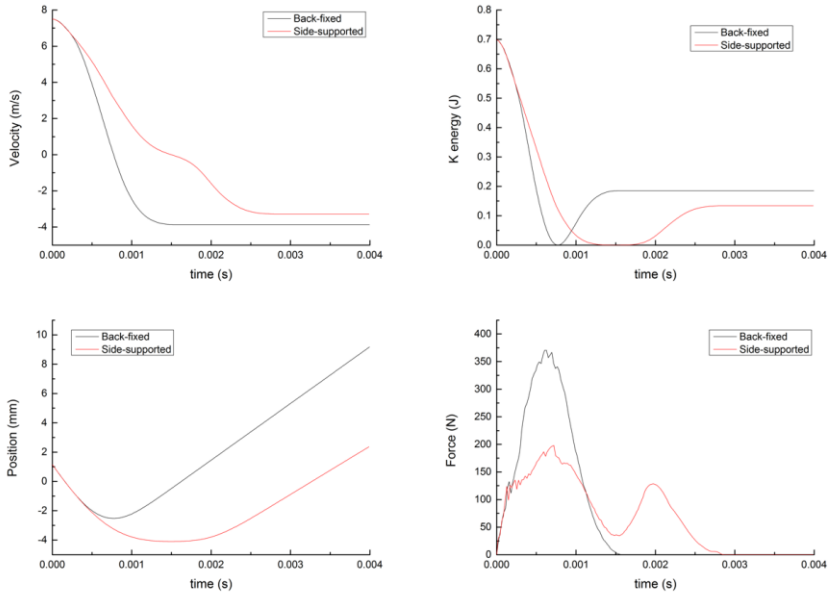

Figure 57. Numerical modeling results of light weight ball (24g & 0.66J Impact Energy) free drop impact to layered TPO/foam panel

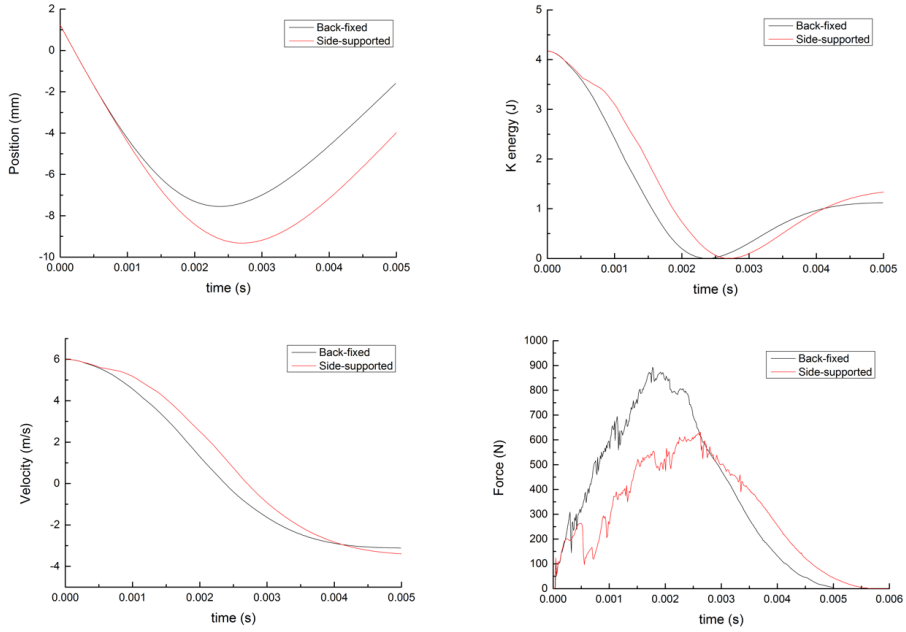

Figure 58. Numerical modeling results of heavy weight ball (240g & 4.2J Impact Energy) free drop impact to layered TPO/foam panel

Chapter 5. Conclusions and Future Work

This dissertation work has focused on the important low-velocity impact phenomenon on layered foam composite panel and provide a quantitative understanding of dominant mechanisms through a combination of experimental tests and finite element simulations. The impact mechanical behavior associated with single-ply thermoplastic polyolefin roofing membrane was examined as an engineering application. It has the potential to sustain the hail impact loads sufficient for maintaining the structural integrity of the structure for velocities up to 40m/s. For a small scale roofing system panel, a quarter-symmetry FEM model was created in order to compare numerical simulations with controlled impact tests. A good correlation between the finite element simulation and controlled velocity indentation test was observed.

Material properties obtained from measurements at loading between 5mm/s to 70mm/s were used to predict the impact response of the layered composite system at higher impact velocities e.g. 0.1m/s to 40m/s. A finite element model was created and was utilized to predict the failure mechanisms in a model roofing system subjected to low velocity hail impact. A good correlation between the finite element simulation and constant velocity indentation tests were observed. Currently, high-velocity in a range of 35m/s to 45m/s ice-ball impact experiments are being conducted in an effort to compare the finite element model with experimental measurements. It is anticipated that these results will depend not only on the diameter and velocity of the ice-ball, but also on the boundary conditions imposed on thee composite test panel. Additional simulations can

be done to capture the mechanical response of the layered foam composite panel under different shapes of the impactor and supporting boundary conditions. The deflection results from the finite element simulation of the layered roofing system application can be used to compare with addition ice-ball impact tests for further examination.

Bibliography

[1] Shim, V. P. W., V. B. C. Tan, and T. E. Tay. "Modelling deformation and damage characteristics of woven fabric under small projectile impact." International Journal of Impact Engineering 16.4 (1995): 585-605..

[2] Lee, B. L., et al. "Penetration failure mechanisms of armor-grade fiber composites under impact." Journal of Composite Materials 35.18 (2001): 1605-1633

[3] Lim, C. T., V. B. C. Tan, and C. H. Cheong. "Perforation of high-strength double-ply fabric system by varying shaped projectiles." International Journal of Impact Engineering 27.6 (2002): 577-591

[4] Cunniff, P. M. "Dimensionless Parameters for Optimization of Textile-Based Body Armor Systems.

[5] Venkataraman, S., and Raphael T. Haftka. "Structural optimization complexity: what has Moore's law done for us?." Structural and Multidisciplinary Optimization 28.6 (2004): 375-387

[6] Ramakrishna, S., Zheng Ming Huang, and H. M. Yew. "Development of a novel flexible composite material." Journal of Materials Processing Technology 89 (1999): 473-477

[7] Avalle, Massimiliano, Giovanni Belingardi, and R. Montanini. "Characterization of polymeric structural foams under compressive impact loading by means of energy-absorption diagram." International Journal of Impact Engineering 25.5 (2001): 455-472.

[8] Roylance, David. "Stress wave propagation in fibres: effect of crossovers." Fibre Science and Technology 13.5 (1980): 385-395.

[9] Cunniff, Philip M. "An analysis of the system effects in woven fabrics under ballistic impact." Textile Research Journal 62.9 (1992): 495-509.

[10] Roylance, SS Wang; Penetration mechanics of textile structures. RC Laible (Ed.), Impact and Phenomena 5, Elsevier (1980)

[11] Banhart, J. (2001). Manufacture, characterization and application of cellular metals and metal foams. Progress in Materials Science, 46(6), pp.559-632.

[12] Peroni, M., Solomos, G., Pizzinato, V, "Impact behavior testing of aluminum foam," Int. J. of Impact Engineering, 53, (2013).

[13] Mesarovic, Sinisa Dj, and Norman A. Fleck. "Spherical indentation of elastic–plastic solids." Proceedings of the Royal Society of London A: Mathematical, Physical and Engineering Sciences. Vol. 455. No. 1987. The Royal Society, 1999.

[14] Avalle, Massimiliano, Giovanni Belingardi, and R. Montanini. "Characterization of polymeric structural foams under compressive impact loading by means of energy-absorption diagram." International Journal of Impact Engineering 25.5 (2001): 455-472.

[15] Zhao, H., G. Gary, and J. R. Klepaczko. "On the use of a viscoelastic split Hopkinson pressure bar." International Journal of Impact Engineering 19.4 (1997): 319-330.

[16] Shockey, Donald A., David C. Erlich, and Jeffrey W. Simons. Improved barriers to turbine engine fragments: interim report III. SRI INTERNATIONAL MENLO PARK CA, 2001

[17] Callister, William D., and David G. Rethwisch. Materials science and engineering: an introduction. Vol. 7. New York: Wiley, 2007.

[18] Cheeseman, Bryan A., and Travis A. Bogetti. "Ballistic impact into fabric and compliant composite laminates." Composite Structures 61.1 (2003): 161-173.

[19] Roylance D, Wilde A, Tocci G. Ballistic impact of textile structures. Text Res J 1973;43:34-41.

[20] Walsh, T. F., B. L. Lee, and J. W. Song. "Penetration failure mechanisms of woven textile composites." PROCEEDINGS-AMERICAN SOCIETY FOR COMPOSITES. 1996

[21] De Morais, W. A., S. N. Monteiro, and J. R. M. d'Almeida. "Effect of the laminate thickness on the composite strength to repeated low energy impacts." Composite structures 70.2 (2005): 223-228.

[22] Parga-Landa, B., and F. Hernandez-Olivares. "An analytical model to predict impact behaviour of soft armours." International Journal of Impact Engineering 16.3 (1995): 455-466.

[23] Zhang, Jun, et al. "Constitutive modeling of polymeric foam material subjected to dynamic crash loading." International journal of impact engineering 21.5 (1998): 369-386.

[24] Shah, Qasim H., and Ameen Topa. "Modeling large deformation and failure of expanded polystyrene crushable foam using LS-DYNA." Modelling and Simulation in Engineering 2014 (2014)

[25] Nelson, Thomas, and Erke Wang. "Reliable FE-Modeling with ANSYS." Proceedings of the International ANSYS Conference. 2004.

[26] Kim, Jang-Kyo, and Yiu-wing Mai. "High strength, high fracture toughness fibre composites with interface control—a review." Composites Science and Technology 41.4 (1991): 333-378.

[27] Iannucci, L., et al. "A failure model for the analysis of thin woven glass composite structures under impact loadings." Computers & Structures 79.8 (2001): 785-799.

[28] Taylor T.J., and Yang L.-Y., Physical Testing of Thermoplastic Polyoflefin Membranes and seams", Interface: membranes, pp. 4-9

[29] Mooney, M. "A theory of large elastic deformation." Journal of applied physics 11.9 (1940): 582-592

[30] Ogden, R. W. "Large deformation isotropic elasticity-on the correlation of theory and experiment for incompressible rubberlike solids." Proceedings of the Royal Society of London A: Mathematical, Physical and Engineering Sciences. Vol. 326. No. 1567. The Royal Society, 1972

[31] Rivlin, R. S. "Large elastic deformations of isotropic materials. II. Some uniqueness theorems for pure, homogeneous deformation." Philosophical Transactions of the Royal Society of London A: Mathematical, Physical and Engineering Sciences 240.822 (1948): 491-508

[32] Sussman, Theodore, and Klaus-Jürgen Bathe. "A finite element formulation for nonlinear incompressible elastic and inelastic analysis." Computers & Structures 26.1 (1987): 357-409

[33] Bažant, Zdeněk P., and Milan Jirásek. "Nonlocal integral formulations of plasticity and damage: survey of progress." Journal of Engineering Mechanics (2002)

[34] J. Payne. "Low Velocity Impact Behavior and Modeling of Loose-Knit Polymer Composite Materials" Ph.D. dissertation, Lehigh University, (2013)

Appendices

Table 3. TPO membrane Mooney-Rivlin Parameters

Material Properties	Symbol	Thermoplastic Olefin
Density	ρ (kg/m^3)	983.7
Mooney-Rivlin C10		-154.78
Mooney-Rivlin C01		168.68
Mooney-Rivlin C20		916.43
Mooney-Rivlin C11		-2436
Mooney-Rivlin C02		1709.4
Incompressibility Parameter D1		0

Table 4. Crushable Foam Model Parameters

Material Properties	Symbol	Fiber yarn
Density	ρ (kg/m^3)	315
Young's Modulus	MPa	401
Poisson's Ratio		0.03
Maximum Tensile Stress	MPa	160

Table 5. Relationship of Impact Velocity and Kinetic Energy of 2-inch diameter ice-ball

2 inch diameter ice ball, 60g weight	
Impact Velocity (ft/s)	Kinetic Energy (J)
130	48.3
110	33.2
90	22.6
70	13.6

Vita

Tianyi Luo was born on December 30, 1984 in Shenyang, Liaoning Province, China. He is the son of Fengming Luo and Qi Li. Tianyi began his studies at Beijing University of Technology in Beijing, China. He graduate with a Bachelor of Science Degree in Mechanical Engineering. After that, he attended Lehigh University for his graduate studies. He worked as a research assistant at Lehigh Energy Research Center and earned his Master of Science Degree in Mechanical Engineering under Sc.D. Edward K. Levy in January 2011. In January 2013, Tianyi started pursuing his Ph.D in Mechanical Engineering of Lehigh University while working as a research assistant under Dr. Herman F. Nied. Tianyi had worked as a Packaging Engineer Intern at Texas Instruments Lehigh Valley during school summers. Tianyi's current research interests are in the fields of finite element modeling, characterization and dynamic simulation of composite materials, and electronic IC packaging design and analysis.